ABSTRACT

EXAMINATION AND MATHEMATICAL MODELLING OF SHRINKAGE RATE OF UNIFORM DROPLETS IN A MICROFLUIDIC SYSTEM DESIGNED FOR BIOPRESERVATION

Ufuk OKUMUŞ

Master of Science, Department of Chemical Engineering

Supervisor: Ass. Prof. Selis ÖNEL

January 2015

Biopreservation is a method currently used in clinical medicine, tissue engineering, food industries, cosmetics and is growing in use in many research platforms. There are several techniques used to achieve satisfactory preservation of mammalian cells. Lyopreservation (dry-preservation), hypothermic preservation (low temperature) and cryopreservation (very low temperature below 77K) are examples of biopreservation methods. Cryopreservation is the most popular and successful method among these techniques. Nevertheless, there are some downsides in cryopreservation for mammalian cells which are not able to endure very low temperatures naturally.

In any preservation method, essential mechanism is decreasing the mobility of the intracellular molecules. Decreasing temperature is one way to achieve immobility. The underlying reason for using immobilization is the excessive osmotic pressure caused by intracellular molecules when they start to crystallize at low temperatures. During freezing, crystallization can cause fatal damage to cells by pushing mobile molecules and confine them in small bits of cell volume causing dramatic decrease in local ion concentration eventually result in poisoning of cell organelles. In addition to this phenomenon so called 'solute trapping', crystallization can

cause physical damage to cells by expansion during freezing as well as sharp tips tearing cell membrane. Crystallization is the basic problem for cryopreservation and it can be prevented if molecular mobility is decreased. The state where molecules are immobilized (solidified) without forming crystals is known as the glass like form 'vitrification'. In order to achieve vitrification tremendous rates of heat removal must be applied on cells around 10^{-6} C/s which are currently not possible for biological materials. Tardigrade, a self-preserving microorganism, can solve this crystallization and heat removal problem by replacing its cytoplasm with trehalose molecules and increasing glass transition temperature of its cytoplasm. Currently, very same method is used in cryopreservation protocols to achieve vitrification in mammalian cells which are not self-preserving. Molecules similar to trehalose called cryo-protective agents (CPAs) are used for such purposes to prepare cells for cryopreservation. CPAs simply decrease molecular mobility in the cytoplasm by intervening water molecules and make it possible to vitrify cytoplasm at reasonable heat removal rates.

Although CPAs are very helpful for adjusting heat removal rates, there are some critical issues to be considered while preparing cells for biopreservation via CPAs. Mammalian cells are not naturally adaptable to CPAs especially at high concentrations. Cells can endure CPA concentrations >6M just for couple of minutes and can endure longer at lower concentrations. Another issue in the current cryopreservation protocol is the osmotic effects caused by CPAs. CPAs are loaded into the cells starting at low concentrations and increased step by step to higher concentration by replacing cell into higher concentrated CPA solutions in every step. Although mammalian cells can stand this process, all the mechanical and osmotic stress on the cell decreases the viability of the cells.

In this thesis we investigated a new method via microfluidic devices proposed by Dr. Mehmet Toner for pre-concentration of cells with CPAs while putting cells under a lot fewer mechanical and osmotic stresses than traditional methods. New method is based on trapping cells into aqueous droplets and controlling the CPA concentration in the droplet by adjusting temperature of the system. An organic phase which can solve small amounts of water, yet immiscible with water is utilized as the bulk fluid. Promoting effect of temperature on solubility is used to adjust water solubility of organic phase. Water is directed into organic phase with additional utilization of convective mass transport via fluid flow resulted gradual

increase in CPA concentration within the aqueous droplet and the mammalian cell trapped in the droplet. By conducting Finite Element Analysis calculations, we found that it is possible to pre-concentrate mammalian cells with CPA 10 times the initial CPA concentration under 3 minutes with the new BioMEMS based method.

Nomenclature

Latin:

A: Area

B.C: Boundary Condition

C: Concentration

CPA: Cryoprotective Agent

D: Diffusion Coefficient

f: Body Forces

J: Flux

k: Convective Diffusion Coefficient

l: Characteristic length

L: Length

L_p: Hydraulic Conductivity

N_{RE}: Reynolds Number

N: Mass

N_s: Solute Amount

N_{Sh}: Sherwood Number

P: Pressure

P_s: Solute Permeability

R_i: Radius (equal to y-coordinate on **eq.3**)

R: Universal Gas Constant

T: Temperature

t: time

u: Relative Velocity

Ui: Aqueous droplet velocity

v: linear velocity

V: Volume

V_w: Water Volume

w: Width

x: Distance

Δx: Cell Membrane Thickness

Greek:

μ: Viscosity

π: Osmolality

ρ: Density

σ: Fluid Stresses

Subscripts denote, s: Solute, i: Time dependent (at any time), 0: Initial, f: Final

Superscripts denote, e: extracellular, i: intracellular

Contents

1. Introduction

Preservation and long term storage of cells is an essential need for many emerging cell based technologies. Many and more cells are being preserved in clinics and labs for research and medical applications. There are different techniques to preserve a cell but they are referred as 'biopreservation' for generally speaking (Acker 2007). Biopreservation can be expressed as; reversibly interrupting and suspending the vital activity of a living organism to hold stored in its non-native environment and vitalize it back later when organism is wanted to be biologically active again (M. Toner 2005). It is a naturally developed process by some microorganisms, however not naturally occurring in mammalian cells. Since mammalian cells are the smallest pieces of mammalian organs and systems, they are in great importance for reparative medicine related research. For instance tissue engineering applications are mostly dependent on the cells and cell behaviors. (Acker 2007) Without preserved and cultured mammalian cells the only option to study on mammalian cells is the experiments on animals which are expensive and very limited. Hence, in vitro mammalian cell lines are created and widely being used today.

There are several techniques to perform biopreservation. Some of them are hypothermic or cold preservation at relatively high (~4C) temperatures, cryopreservation at very low (cryo) temperatures and desiccation (drying) at room temperature (Hammerstedt, Graham et al. 1990, Rubinsky 2003). All these techniques are focused on disabling chemical activity within the cell. The preferred preservation method is chosen by the criteria: How long the preservation will last, what kind of cell is going to be preserved or what the purpose of the preservation is. As matters stand, cryopreservation come to the forefront as the most reliable and favorable technique for biopreservation of mammalian cells. In this project, we focused on cryopreservation application and transport mechanisms within micro-channels through application of preservation of mammalian cells.

A mammalian cell is consisting of organelles, a core with genetic material, cytoplasm and a membrane keeping everything inside. Cytoplasm content is mostly water allowing all the molecules within the cell to move freely for necessary chemical interactions to maintain vital activities. In a broad sense, 'water' or the 'cytoplasm' is the connection material between the

organelles, core and outer environment of the cell. From this point of view, if water is immobilized or completely removed from the cell, all the chemical activities, hence the vitality of the cell would be suspended. However, the immobilization process is possible only if certain conditions are provided (Michael J. Taylor 2004). One important condition is rapid cooling. It is possible to vitrify water if very high and costly rate of cooling ($\sim 10^{-6}$C/s) is applied. Such cooling rates are currently not possible for biological materials. But, there is a way around this restriction by use of cryoprotectant agents (CPAs). CPAs are biocompatible substances which penetrate between water molecules and limit the mobility of the water molecules. As a result, water can be immobilized at lower cooling rates than 10^{-6}C/s.

In order to understand the underlying mechanism in vitrification, molecular mobility of water molecules and other ions in the cytoplasm must be studied. When cooling is under progress, if the mass transfer rate of water within the cell is high, then the cell will most likely suffer dehydration. If mass transfer rate of water is low enough, which is possible with ultra-fast cooling, then the cell cytoplasm can undergo vitrification suspending the mobility of any intracellular molecule (A. Aksan and M. Toner (M. Toner 2005)).

This research significantly involves microfluidics technology. Bio Micro Electro Mechanical Systems (BioMEMS) technology is better than just an emerging technology now. It is being widely used in medicine, biotechnology, tissue engineering, electronics, qualitative analysis and many other researches related to health science or not (Ho, Lin et al. 2006, Chiu 2007, Jeffries, Kuo et al. 2007, Song, Moon et al. 2009, Sgro and Chiu 2010, Prot, Bunescu et al. 2012, Swain, Lai et al. 2013). They are easy to monitor and control, since small micro-channels and micro-wells are the only sections where reactions and physical changes take place. Also they are continuous systems that are allowing engineering solutions for production of chemicals, detection of trace amounts and examination of small droplets and reaction containers (Chiu 2007, Chiu, Lorenz et al. 2009).

In this study we focused on mathematical modeling of mass transfer in micro-droplets that are utilized for pre-treatment of cells before cryopreservation. Small micro-channels are capable of carrying cell containing aqueous droplets in an organic phase (He, Edgar et al. 2005, Chiu 2007, Chiu and Lorenz 2009), where, organic phase is a phase immiscible with water, yet has a capacity to solve water in small amounts. Changes in the temperature promote the solubility

of water in organic phase, hence, allow us to control mass transfer of water between aqueous droplet and organic phase by controlling heat transfer (Bajpayee, Edd et al. 2010, Kuo and Chiu 2011). Here we make use of water loss of the aqueous droplets simply because decreasing water amount in a closed system increases the concentration of the remaining molecules. The important advantage of using continuous flow in a micro-device is, the increase in the concentration is a continuous and controlled change rather than a step change which harms mammalian cells by osmotic effects (Song, Moon et al. 2009, Heo, Lee et al. 2011). This method is proposed to increase the viability of the cells after cryopreservation (Bajpayee, Edd et al. 2010, Heo, Lee et al. 2011).

Microfluidic devices have many advantages. However, manufacturing a microfluidic device needs good preparation and fine predictions. Arrangement of the channels and other attributes can be tricky most of the time. Any mistake made during the design of the micro-device can conclude in loss of important sources. Mathematical and software modeling of multi-physical systems can ease the manufacturing process. Moreover, it can allow scientists to make good predictions over the system and test many parameters during device design process without spending precious sources. Modeling can provide opportunity to step in before producing deficient designs. Also it can give a scientist means to check experimental data with the mathematical calculations and create more controlled and methodical work. In this project we constructed a detailed model of a microfluidic device originally created by the researchers of BioMEMS Resource Center and Center for Engineering in Medicine under supervision of Dr. Mehmet Toner. The device consists of two transparent rectangular micro-channels which are arranged to intersect and create a T-junction where the droplets are formed and directed into a wider channel as seen on **figure.3.2** and **figure 3.4**. We investigated Transport Phenomena and fluid flow within the channel in which the cell containing aqueous droplets are flowing suspended within the organic phase. COMSOL Multiphysics software is used to create multi-physic models and MATLAB® is used to support and add extra mathematical expressions needed for the model. These software are processed simultaneously to obtain the eventual model. AutoCAD Engineering Design software is used to create the geometry of the system. With regard of our model and experimental observations we proposed microfluidic device model including design parameters for pre-treatment of mammalian cells before

cryopreservation. We believe our model will be a nice step to define various microfluidic systems in detail.

2. Theory

Microfluidics is a multidisciplinary research field and researchers must possess knowledge in numbers of disciplines varying from fundamental physics to biology, electronics to chemistry. Design, shape and device material may completely change depending on purpose of use of the microfluidic device. Working principles of these devices can be very similar or can be very distinctive. In recent years, microfluidic devices are involved in many researches in many areas minor and major. It can take years of work to completely understand all types of devices. Here in this thesis BioMEMS (Bio micro electro mechanical systems) and Bio-preservation oriented devices will be emphasized with an analyzed application of single cell droplet microfluidics. Ultimate goal of this research was to create an optimized model for pre-concentration issues faced in cryopreservation of mammalian cells, in addition to creating a point of reference for future micro droplet applications made use in microfluidic devices. Covered topics are nested in groups in this thesis to reflect a better overview of the topic and to create a reader friendly texture.

2.1 System Definition

Figure-2.1 illustrates the system sections where we carried out calculations. We assumed that water diffuses freely through cell membrane with low resistance to diffusion, and that the water amount in the droplets is the sum of water present within the cell and water present out of the cell within the droplet.

Gradually increasing CPA concentration is the main purpose of the method which is tested in this thesis. Continuous increase needed in the CPA concentration is maintained by removal of water from the droplet. All calculations are performed for micro-channel with 150x200µm cross-section and flow regime was always laminar.
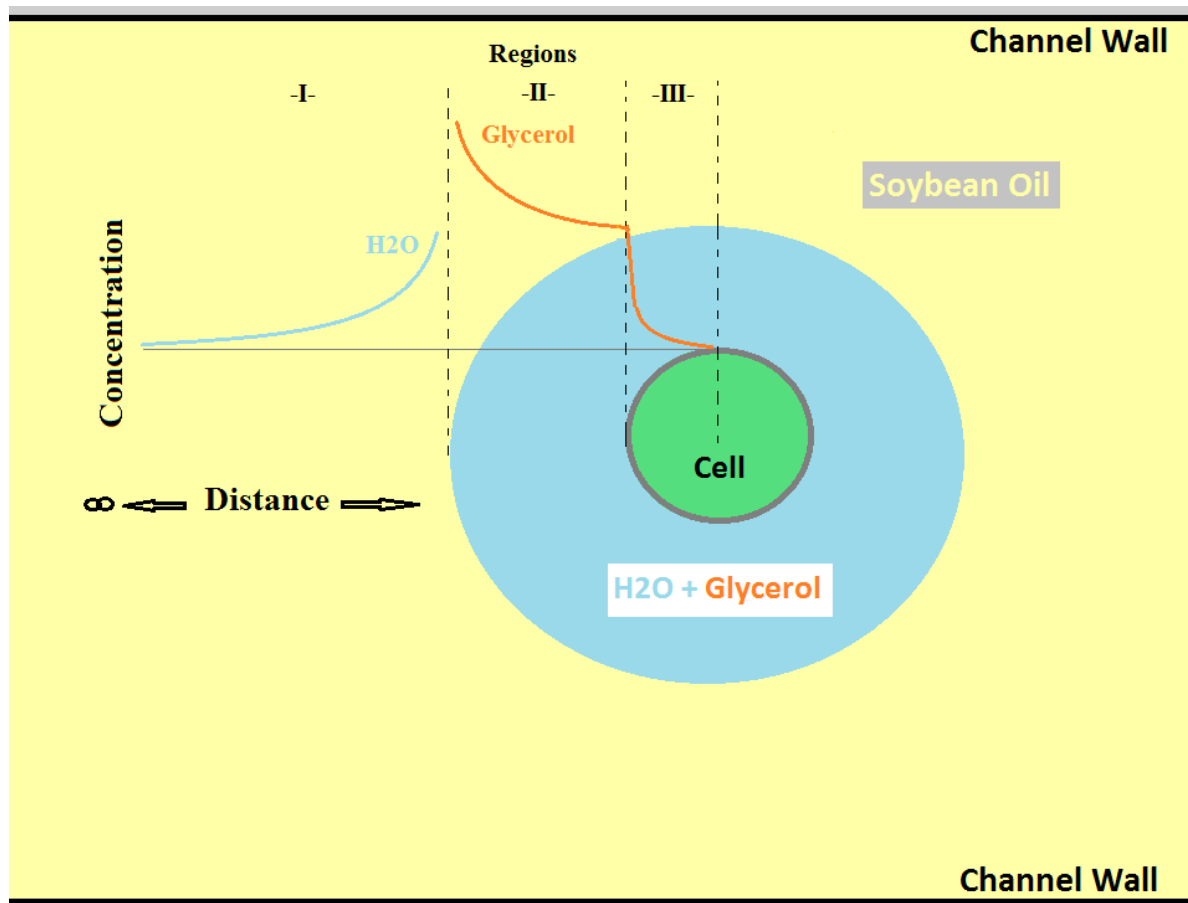
Figure-2.1. A representative figure of the regions that are modeled. Region-I- diffusion of water into organic phase, Region-II- Diffusion of CPA within droplet, Region-III- Diffusion of CPA through cell membrane and inner cell.

Organic phase which is saturated with water at initial operating temperature ($20\ ^{\circ}$C) is introduced into the channel. Hence no net mass transport of water takes place at $20\ ^{\circ}$C. After producing desired droplet formation heat is supplied to system with an electronically controlled heater which can keep system at any temperature between $20\ ^{\circ}$C – $50\ ^{\circ}$C. As system is heated, solubility of water within the organic phase is enhanced, creating a concentration gap, a driving force, for water to diffuse into organic phase. Hence, a system is created where diffusion of water into organic phase is controlled by temperature.

2.2 Microfluidic Devices

Microfluidic devices are originated from various researches in history to maintain certain needs of people. First it came out to carry out molecular analysis methods; gas chromatography (GPC), high pressure liquid chromatography (HPLC) and capillary electrophoresis (CE). These micro-analytical methods have used microfluidic methods to make it possible to carry out high sensitivity analysis with very small amounts of samples. Capillary channels are utilized in these techniques. After achieving successful results researchers sought for improvements and various new applications (Whitesides 2006). One of these applications was developed in molecular biology. Sensitive microanalysis needed for genomics, DNA sequencing, has been partly maintained by microfluidic approaches (Whitesides 2006).

In 1990s, US Department of Defense has supported various researches on microfluidic devices to develop mobile detectors to protect their members in the field against chemical and biological threats. Co-operations with academy resulted in significant improvements in microfluidics technology (Whitesides 2006).

Another contribution came from silicon microelectronics. Some applications of photolithography and MEMS had been successful when applied to microfluidics in early periods (Czaplewski, Kameoka et al. 2003, Mijatovic, Eijkel et al. 2005). Later use of silicon in microfluidics was found inappropriate and mostly replaced with plastics like PDMS except for the use of silicon in rigid microfluidic device parts such as pumps or valves (Jessamine M. K. Ng 2002, Whitesides 2006).

In recent years, with the evolving technology automated systems with integrated electronic circuits have revolutionized our world from research labs to homes. As we get familiar with these systems a reasonable approach have been developed that if we can automate biological systems too? In fact, utilization of micro-channels is nothing new and microfluidic devices have been growing in importance as we identify more about micro-systems. Underlying physics in microfluidic systems are being widely studied to fulfill this purpose.

Today microfluidic devices are often referred as micro electro mechanical systems (MEMS). After first use of micro-channels on chromatography devices, microfluidic devices have

developed a lot and many other systems have integrated into micro devices. MEMS can be considered as very complicated devices with micro valves, electromagnetic micro tools and often with very complicated micro channel distributions and flow patterns. Of course all these tools have brought a new use for these systems (Weibel and Whitesides 2006, Whitesides 2006).

Development of microfluidic devices are in close relation with lithographical applications. Lithography is the main technique used to manufacture a micro device. Sensitivity level needed for production of micro-channels and micro-tools used within channels can only be achieved with a liable technique like lithography. During manufacture, patterns needed for micro-channels are maintained by use of surface lithography on a silicon wafer, and then molds for casting of structural polymer are produced with high sensitivity by using these patterns. Casting is followed by a vacuum chamber and oxygen plasma on glass surface is used to fix the polymer on the glass slide. Usually several types of poly-dimethyl siloxane (PDMS) are used as polymer material for biological applications. Manufacturing of high pressure micro-devices are also utilizes lithography but since more rigid materials are used in those devices, no molding is applied.

Micro channels naturally have very large surface area to fluid volume ratio compared to industrial macroscopic devices. This phenomenon gives microfluidic devices a characteristic flow pattern severely affected by surface tension. In a micro-channel flow is driven by only viscous forces and yielding flow regime is always perfectly laminar. This occasion causes mixing issues to become a whole new topic to be focused on while bringing a lot of new use for these systems (Stroock, Dertinger et al. 2002). Further information on flow characteristics is given in section **2.4.1** fluid dynamics in micro-channels.

Microfluidic devices are being used for very high velocity applications using silicon and glass as the structural material. High pressure and velocity can be achieved in these systems. Hence, applications towards micro-reactors are often utilized in such systems when pressure increases the selectivity of the yielding reaction product (Elvira, Casadevall i Solvas et al. 2013). However, in this thesis context biological applications are handled rather than industrial high pressure applications.

MEMS that are developed for biological applications, referred as BioMEMS, have been used fields in ranging from cryopreservation to fertilization, proteins to genetic researches (Squires and Quake 2005, Dittrich and Manz 2006, Chiu and Lorenz 2009, Song, Moon et al. 2009). Moreover, droplets generated in micro-channels are considered as single reaction containers and many other applications sensitive to concentration including protein nucleation, crystallization and macromolecular crowding are yet to come for micro droplets flowing in micro-channels (Beebe, Mensing et al. 2002, He, Sun et al. 2004, Chiu 2007, Jeffries, Kuo et al. 2007, Chiu, Lorenz et al. 2009, Bajpayee, Edd et al. 2010, Lagus and Edd 2013).

Mainly, the greatest advantage brought by microfluidic devices is the existence of flow. Biological applications are often conducted on petri dishes where no regular predictable flow can be used. In micro-channels, biological organisms of couple of microns wide can be monitored as accurate as they were in petri dishes with the addition of flow when needed. Occurrence of flow can promote mass transfer greatly, separation can be done with the aid of flow, and a closed environment can be maintained whenever necessary. Two phase flow can be utilized to create precipitations or needed confined areas to perform detailed analysis (Kenis 1999, He, Sun et al. 2004). The only disadvantage of microfluidic devices is the cost of these systems. They usually must be specific to application and usually have a unique pattern for each device. Hence, for now, cost can be a little bit weary. As a result of better identification of physics underneath micro-channels, we hope our research will partly contribute to financial issues.

In our research we created an insight to understand the flow dynamics and mass transfer in microfluidic devices better for droplets generated in micro-channels. There are many issues to be understood in BioMEMS applications like encapsulation of cells into droplets. Also very interesting applications are available with multiple phase flows, electromagnetically driven flows and concentration control with optical vertex (Squires and Bazant 2004, Jeffries, Kuo et al. 2007). We highly encourage any reader to search for MEMS and BioMEMS through literature to understand the possible uses and impacts of these devices.

2.3 Cryopreservation

Cryopreservation, as the most successful preservation method to date, has been used widely as part of cancer and root cell research to protect and store mammalian cells despite complications. The cell cytoplasm that surrounds the organelles is mostly composed of water causing undesired results during freezing, such as expansion, extracellular ice formation, crystallization, and local increase in solute concentration (solute trapping) due to crystallization (Toner, Cravalho et al. 1990). Crystallization and other solute effects can be prevented by vitrification of cell cytoplasm. To achieve vitrification very fast cooling rates (10^6-10^7 C/s) must be exerted. With such high cooling rates water can be vitrified at -135 C. During vitrification, the rate of heat transfer must be so high that it will prevent any mass transfer that would form harmful crystals. Unfortunately, ultrafast cooling is currently not possible for biological materials. Even so, reduction of rate of mass transfer within the cell cytoplasm is possible. Aforementioned damage to the cell can be eliminated by increasing glass transition temperature via introduction of cryo-protectant agent (CPA) carbohydrates such as glycerol into the cell (Meryman 1971, Eroglu, Russo et al. 2000). With the aid of CPAs, ratio of heat transfer rate to mass transfer rate can be held at reasonable levels (M. Toner 2005). This mechanism is naturally being used by some multicellular organisms. 'Tardigrade', an organism that can stand almost any condition, can replace its intracellular water with sugar trehalose and survive freezing by preventing crystallization. However, mammalian cells do not possess such ability. Exposure to high concentrations of CPAs induces toxic effects and causes damage to the cell due to osmotic stresses and shrinkage. To employ cryopreservation, special process must be implemented (Youm, Lee et al. 2014).

Currently, cryopreservation protocols include exposing of cells to relatively sudden changes of CPA concentrations to render them take CPA into cells (Youm, Lee et al. 2014). Cells respond these changes in the way they would damage their organelles causing lethal damage to whole cell in the end. To prevent lethal conditions, cells are taken into CPA solutions step by step. For instance; in the first step, cell is taken into 0.5 M CPA solution and kept there for couple of minutes and then taken into 1M CPA solution and kept there for a while and this process goes on until desired CPA concentration is reached within the cell. In addition to osmotic stress, all these steps put cells under a lot of mechanical stress with use of volume

pipettes. Although yet, mammalian cells can stand all these process, considering additional damage by the toxicity when cells are exposed to CPAs for too long, viability of cells are reduced in considerable amounts during all the rush of the pre-concentration process. A method that puts cells under less osmotic and mechanical stress in optimized time scales would fairly increase viability of cells.
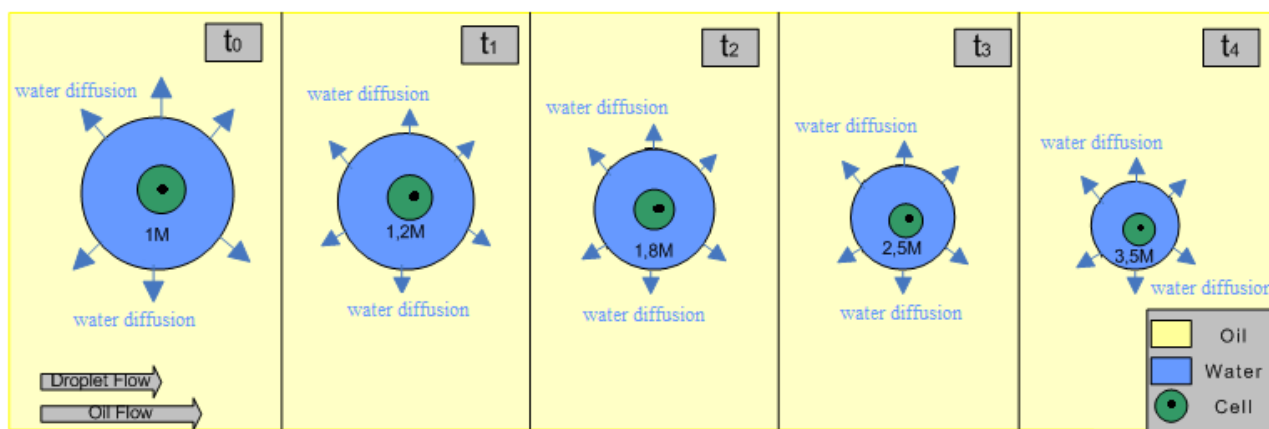

Figure 2.2 - Schematic representation of droplet shrinkage in microfluidic channel and water diffusion into organic phase yielding gradual increase in CPA concentration.

The rate and amount of CPA loading to the cell can be adjusted by controlling the CPA concentration through adjusting the amount of water around the cell. In this research, a CPA loading protocol proposed by Dr. Mehmet Toner is developed by using a thermal micro-channel fluidic system, where controlled continuous increase in CPA concentration profile is enforced. **Figure.2.2** is a schematic representation for proposed method for pre-concentration of cells. The new system allows for encapsulation of cells in an aqueous droplet at low CPA concentration and gradual increase of CPA concentration by removal of water from the aqueous droplet into a continuously flowing immiscible organic phase. Soybean oil is employed as the organic phase due to limited solubility of water (~0.3 % by volume (He, Sun et al. 2004)) that is sufficient to achieve the desired aqueous droplet volume by diffusion of water into the thermally controlled oil.

A comparison can be seen on **figure.2.3** which summarizes application of traditional pre-concentration method (stepwise) and proposed methods (progressive). A smooth transition of

17

CPA concentration will create less potential for damaging cells due to osmotic effects. The distinction of work on figure.2A and figure 2.B is the utilization of droplets to create surrounding (buffer) environment for cells. This occasion decreases the potential of osmotic damages on sensitive cells by starting with a low increase ratio of CPA concentration and
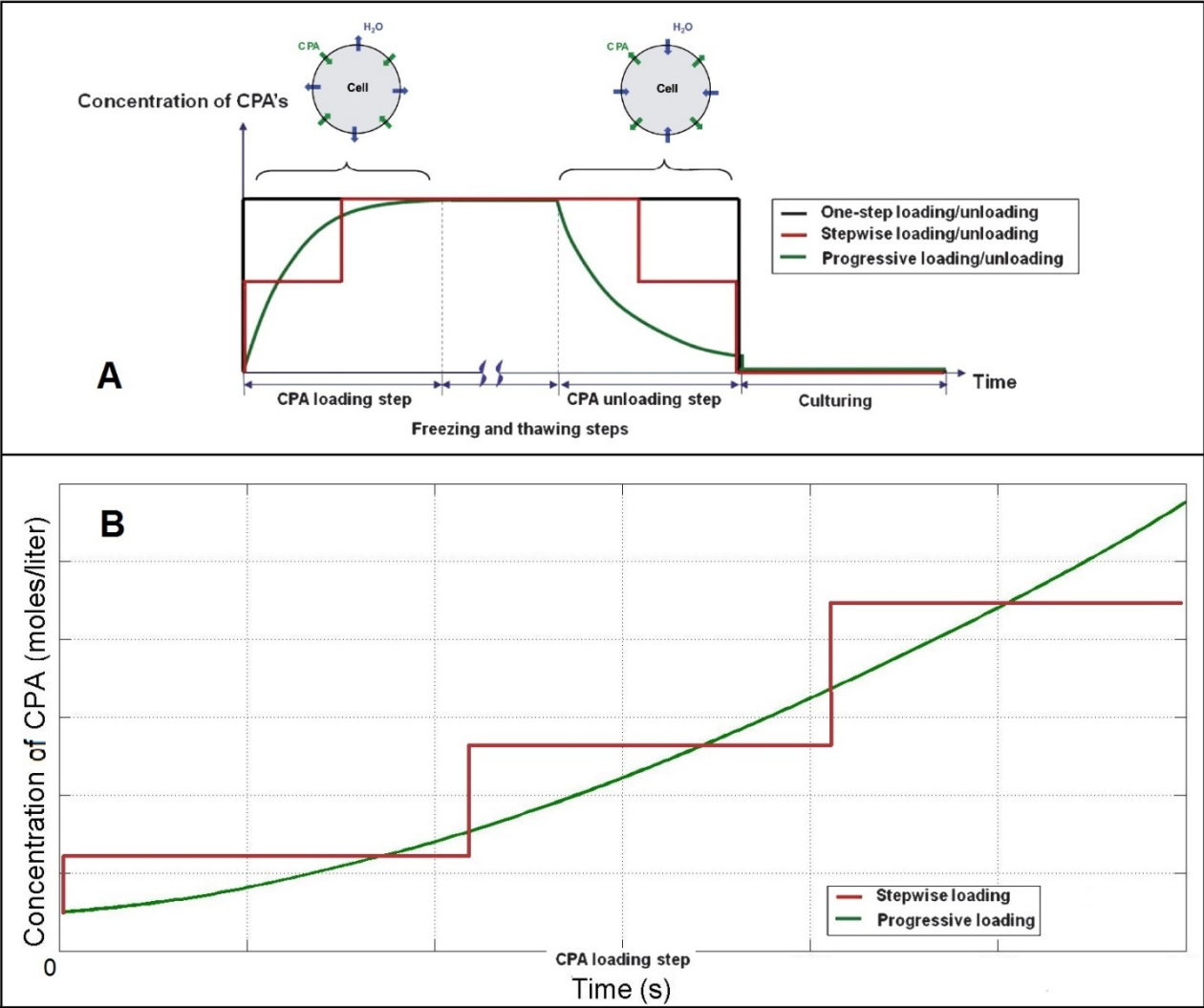
increase gradually with time.

Figure.2.3 – **(A)** Previous work of Utkan Demirci (Song, Moon et al. 2009) describing distinction between stepwise loading/unloading and gradual (progressive) loading/unloading of CPA into cell. **(B)** Distinction between stepwise loading and progressive loading arisen by our work.

2.3 Modeling

In this study, mathematical modeling conducted via finite element analysis method, which is a method used for solving differential equations in limited partitions with respect to given boundary conditions. In this method, a continuous physical problem is divided into very small nodal discontinuous physical partitions (see **figure.2.4**). Each partition is solved with respect to given boundary conditions and found results are chosen as new boundary condition for the neighboring partitions until all system is solved. Step by step, each small sub system is solved by simple convergence functions. Size of the partitions, so called finite elements, determines the sensitivity of the solution. Element size is distributed with respect to needed sensitivity within the physical system. More element count yields more accurate results while it creates a larger work load for processors and takes longer times. Hence, element size and accuracy must be handed well to avoid bad results or long time analysis course up to several days. In our study, finite element analysis calculations are carried on Comsol Multiphysics software. Other calculations of intermediate parameters and curve fits are conducted on MATLAB and MS Excel.
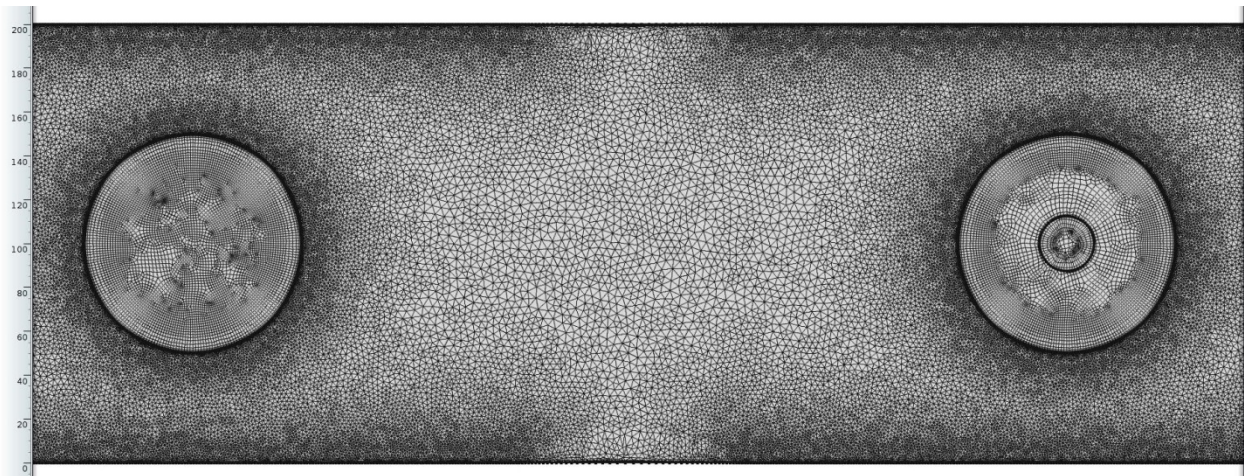

Figure.2.4- A part of the system showing finite elements generated on Comsol Multiphysics software.

Another important factor is the element size quality, also referred as the mesh quality. It is a geometrical measure to define the capability of an element to perform desired calculations. It is scaled between 0 and 1, bad to good respectively. Element quality can be considered as a

measure of how good an element fits into a circle. An element with high quality would fill larger portion of the circle than a lower quality element. This explains the element quality histograms shown on **figure.2.5**. The microfluidic system we modeled has triangular or quadrilateral elements with quality close to 1. Near the boundaries one must use thin quadrilateral elements, which characteristically have low element quality. This is the reason why there are low quality elements on the element quality histogram on the left side of **figure.2.5**. Use of thin boundary layers was a necessity in this study to obtain a robust stretching element for the moving boundary on droplet walls.


Statistics

Complete mesh

Element type: All elements

Triangular elements: 752890
Quadrilateral elements: 189801
Edge elements: 12718
Vertex elements: 76

— Domain element statistics —

Number of elements: 942691
Minimum element quality: 0.006569
Average element quality: 0.805
Element area ratio: 3.325E-4
Mesh area: 1600000.0 μm^2
Maximum growth rate: 12.63
Average growth rate: 1.397

Element Quality Histogram

Statistics

Complete mesh

Element type: Triangular elements

Triangular elements: 752890

— Element statistics —

Minimum element quality: 0.009904
Average element quality: 0.8881
Element area ratio: 0.002271
Mesh area: 1467000.0 μm^2

Element Quality Histogram

Figure.2.5 - Mesh statistics for the calculations.

Transport of Diluted Species module in the Comsol Multiphysics software, which employs **eq.1** and **eq.2**, is used with time dependent, direct solving sequence through the calculations.

COMSOL Moving Mesh module is used to represent the movement of the droplet walls during shrinking.

$$\frac{dC_i}{dt} = \nabla \cdot (D \cdot \nabla C_i) - u \cdot \nabla C_i \qquad \textbf{(eq.1)}$$

$$J_i = -D \cdot \nabla C_i + u \cdot C_i \qquad \textbf{(eq.2)}$$

Where, C: concentration, u: relative velocity, D: diffusion coefficient, t: time, J: Flux, x: distance.

Modeling sequence is started on Comsol first with initial values. **Eq.3 set** is solved in separate software (MATLAB and Excel) and relative velocity 'u' is expressed as a function of 'R' droplet radius.

$$U_i = \left(R_i^2 - \frac{w^2}{4} \right) \cdot \frac{\Delta P}{L \cdot \mu \cdot 2} \qquad \textbf{(eq.3a)}$$

$$u = U_i - U_{avg} \qquad \textbf{(eq.3b)}$$

where, U_i is aqueous droplet velocity, r is radius or y-coordinate, w is width, P is pressure, L is channel length and μ is viscosity, U_{avg} is average organic phase velocity, u is relative velocity.

U value is fed to Comsol calculations at the beginning. With the flux 'J' value output of the Comsol, radius is defined as a function of time denoted as 'Ri'. This loop was necessary to solve the circular dependency of relative droplet velocity on droplet radius, droplet radius on flux, and flux on relative droplet velocity. The calculations are conducted simultaneously, and shown in **figure.4.1** as a flowchart for ease of following. On the second step, where change of radius with respect to time is known, change of CPA concentration within the droplet is calculated as a function of time and distance on Comsol. The important aspect was the cell membrane permeability which was calculated by equations which are currently known as the 2-parameter formalism in the literature, first proposed by Jacobs M.H. in 1932-1933 and revised by Kedem-Katchalsky (Kedem and Katchalsky 1958, Kleinhans 1998, Elmoazzen,

Elliott et al. 2009). Equations are given as **eq.11** and **eq.12** in the Transport Phenomena section.

One of the goals of this research was to find the intracellular CPA concentration at any time at any point in the cell. That value is represented as $C_{intracellular}$ on **figure.4.1** and found as a function of time and location. On the next step all the data is gathered to find an optimum time, droplet size and average velocity to achieve the desired intracellular CPA concentration within mammalian cells via microfluidic devices. All the outcomes of the calculations are presented in the Results section.

2.4 Transport Phenomena

In this research, all the aspects of transport phenomena are considered in detail. The only exception was the heat transfer resistance created by the microfluidic channel walls. Although heat transfer is the key to control mass transfer, calculation of heat transfer rate on micrometer scale does not create any convenience for this research. For fluids flowing in micro-channels, an instant heat up from 20 C° to 45 C° assumption is made considering very small heat capacity of the phases flowing in 150 μm x 200 μm cross section channel. The temperature has always been taken into account when defining mass and momentum transfer parameters. All the initial conditions and unsteady state mass and momentum transfer calculations are chosen or performed considering the temperature effects at 20 C° (lowest) and 45 C° (highest).

Flow characteristics of fluids running through a rectangular channel may vary depending on the dimensions of the channel. Fundamentals of fluid dynamics in large channels are pretty much realized now. In micro scale, fundamental physics may act different than that in large scale observations (Squires and Quake 2005, Janasek, Franzke et al. 2006). The effect, thus, the importance of inertial forces is much higher than viscous forces in large scale systems. This phenomenon allows fluid to mix easily with eddies and turbulence. In microsystems, fluids do not mix convectively. Viscous forces override in significance. Chaotic mixing within the fluid flow is not at stake. For such liquids like water, laminar flow forms and maintains itself within the micro-channel. Occurrence of continuous laminar flow requires specific equipment to perform mixing within the micro-channel. Nevertheless, laminar flow has many advantages in various applications of microfluidic systems (Santiago 2001, Whitesides 2006).

Flow characteristics of a Newtonian fluid can be described by the Navier-Stokes equation given by **eq.4**, which is basically the continuum version of Newton's law of motion, F = m.a, on a per unit volume basis.

$$\rho\left(\frac{\Delta u}{\Delta t} + u \cdot \nabla u\right) = \nabla \cdot \vec{\sigma} + f = -\nabla p + \mu \nabla^2 u + f \qquad \textbf{(eq.4)}$$

Where, u represents the velocity field, t time, σ fluid stresses, f body forces, μ viscosity, ρ density and p pressure. For microfluidic devices where $N_{RE}<1$, inertial forces, thus, nonlinear terms, are negligible and viscous forces dominate fluid characteristics (Squires and Quake 2005). Hence, *Stokes Equation* can be written as;

$$\rho\frac{\Delta u}{\Delta t} = \nabla \cdot \sigma + f = -\nabla p + \mu \nabla^2 u + f \qquad \textbf{(eq.5)}$$

Noting that for incompressible Newtonian fluids with constant density the continuity equation is given by, $\frac{\Delta \rho}{\Delta t} + \nabla \cdot (\rho u) = 0$.

Reynolds Number, N_{RE}, a generalized dimensionless mathematical expression to describe fluid flow characteristics is given by **eq.6**

$$N_{RE} = \frac{l \cdot v \cdot \rho}{\mu} = \frac{F_{initial}}{F_{viscous}} \qquad \textbf{(eq.6)}$$

Where l is the characteristic length, v is linear velocity, ρ is density and μ is viscosity. Together in this form they represent the ratio of initial forces over viscous forces.

When Reynolds Number is very low (<1), the flow is very predictable. The role of inertial forces in this phenomenon is explained by E.M. Purcell excellently in his speech in 1976 (Purcell January 1977) where he compares a human and a bacteria moving in water and the distance they move after removing the forces acting on the two bodies. The bacterium moves 0.1Å due to the lack of inertial forces that would drag it. Same analogy is valid for molecules flowing in a fluid. When no other forces are exerted, no significant inertial forces means no flow. When small forces are applied on the fluid and laminar flow is formed, fluid flows under

the control of these forces and undisturbed by the initial forces. Hence a very predictable, linear and neat laminar flow is formed (Beebe, Mensing et al. 2002). Consequently, flow is 99.9% laminar in microfluidic systems.

Mixing or turbulent flow can often be very desirable. As well known by chemical engineers, mixing is in paramount importance for reactions. Microfluidic devices are often used as micro-reactors for drug industries and for many fine chemical and biological processes (Dittrich and Manz 2006, Chiu 2007, Teh, Lin et al. 2008, Kuo and Chiu 2011). Special equipment or specially designed micro-channels are used to provide mixing for such operations (Beebe, Mensing et al. 2002, Jessamine M. K. Ng 2002, Stroock, Dertinger et al. 2002, Kuo and Chiu 2011). Another important aspect to be considered before wildly mixing substances is, separation of the substances to be sorted or analyzed later. Products of the reactions often needed to be separated and sadly, more you mix harder you separate (Squires and Quake 2005). Then, one should realize that mixing and dispersion issues are in great importance for microfluidic devices. Here in this research, a better feature of what is going on within the micro-channels is tried to be explained by building mathematical models of micro-channels.

For controlled systems, in a broad sense, some parameter(s) is/are kept in their maximum possible value and the other(s) are used to control the process rate. For example, a reacting system can be limited by two parameters: Reaction rate and diffusion rate. If our system was a reacting system, we would want it to be reaction limited since the reaction rate is controllable through temperature. In our microfluidic system, diffusion is wanted to be hold at its maximum value, while temperature is employed to control the diffusion rate. However, in a microchannel, the absolute flow character is laminar flow, which does not allow mass transport to be kept in its maximum possible value. Higher mass transport rate can be achieved by utilizing convective mass transport which is only possible with creation of velocity difference between substances.

In our system, there are two phases flowing together and one phase is suspended in the other. So, although there is laminar flow, convective mass transport from water to organic phase is achieved in the surface of the droplets. Convective diffusion is in great importance compared to molecular diffusion, and it is the dominant component of overall mass transport.

We take advantage of convective mass transport to promote overall diffusion of water into the organic phase. Local convective mass transport takes place over the droplet surface within the liquid-liquid interface. Although organic phase flow is laminar, the liquid-liquid interface, where two liquids are flowing with different velocities, provides satisfactory flow condition that is required for convective mass transport to be formed. Local convective transport of water into the organic phase is effective, but diffusion of water from aqueous droplet to channel walls, perpendicular to flow direction, through the organic phase, will be as slow as molecular diffusion due to laminar flow (see **eq.1** and **eq.2**). Convective effects will not be perceivable for transport of water through the organic phase where net bulk flow velocity of water molecules in the organic phase is zero. That is why one should be sure that sufficient amount of organic phase is presented into the micro-channel to keep diffusion of water through organic phase at a reasonable level by keeping concentration gradient high and remove water from the aqueous droplets efficiently. Aforementioned less active mass transport is sometimes helpful because if it was too fast, the concentration would be increased so fast and the cell might get damaged due to sudden osmotic pressure increase. For droplets larger than 0.5µm and glycerol concentration up to 6M, diffusion rate of water within the aqueous droplet is much higher than the diffusion rate of water through the organic phase (Bajpayee, Edd et al. 2010). This indicates that the transport of water through the organic phase is the limiting factor in our system and our operating range. Even if the temperature is increased suddenly, response of the organic phase to temperature adjustments would be slow which prevents osmotic pressure injury on cells.

In this thesis context, the important aspect to be focused on regarding fluid flow is the fluid-fluid interface region, which is the region where two fluids flow side by side with a velocity difference and create a potential for convective transport of the species. This research is mainly based on the outcomes of velocity difference between the droplets and average organic phase flow velocity. That is a required condition to apply convection-diffusion equation for mass transport on a system. One can observe in **figure.2.6** that as the droplet size decreases, droplets are dragged into the faster regions of the fluid flow profile. Thus, the velocity difference between the droplets and the average organic phase flow velocity changes through time.
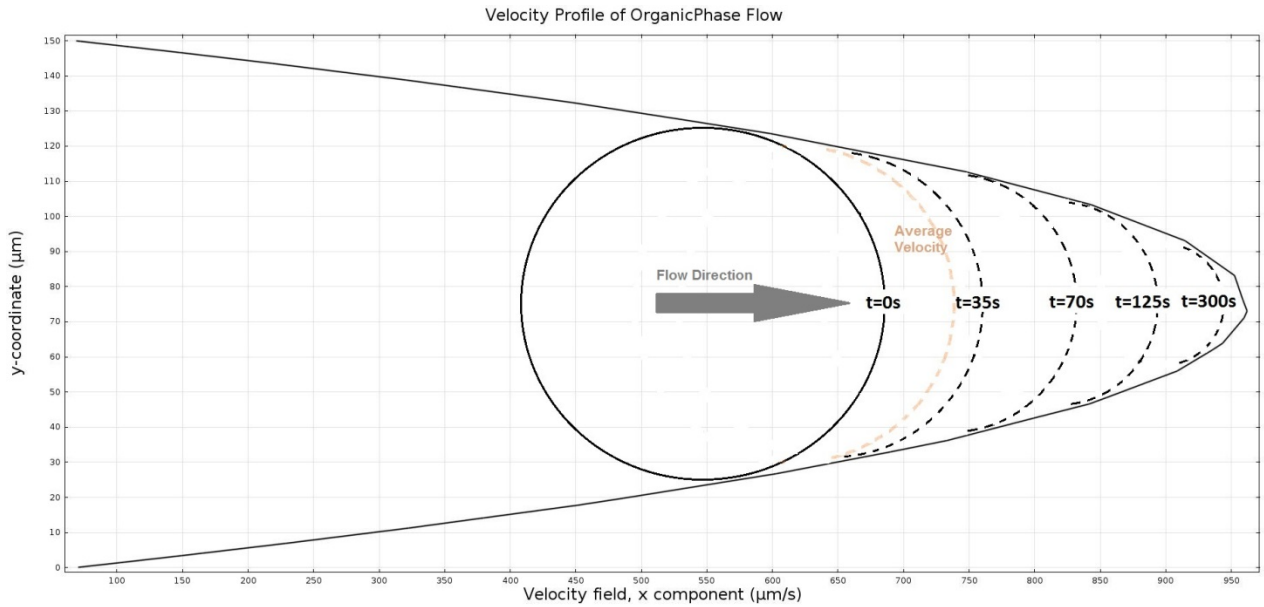
Figure.2.6 – A 100 micron droplet position shown on the velocity profile of the organic phase at 683μm/s flow rate. As the aqueous droplet shrinks, it is dragged into faster regions of the velocity profile. Dashed lines are visionary droplets at mentioned times. Orange line represents average velocity.

A large droplet with R>R$_{critical}$ at the beginning, flows slower than the average organic phase velocity. As water diffuses into the organic phase and the droplet shrinks, it enhances its pace. First it reaches the flow speed of the average organic phase at R=R$_{critical}$, and then keeps accelerating until water diffusion is ceased at an equilibrium state of concentration where R<R$_{critical}$. At R=R$_{critical}$ only diffusive mass transfer takes place. Hence water mass transport rate drops dramatically in the meanwhile until droplet velocity passed average organic phase flow speed. In this thesis, this retarded mass transfer state is entitled Critical Radius State and the Radius in that interval is entitled as R$_{critical}$. Also, according to continuity equation, average velocity of the bulk fluid should be taken into account in order to calculate amount of mass transferred. Average velocity of the organic phase (bulk flow) does not change in the process.

For N$_{RE}$ is less than 1, with laminar flow in the channel, the droplet will always be positioned in the center of the channel width (y-axis). The flow profile seen on **figure.2.6** is based on **eq.3a** derived from equation of motion (R. Byron Bird).

Mass transfer and momentum transfer in this system cannot be considered separately because, fluid velocity enhances convective mass transport and as the mass transport takes place, droplets shrink and accelerate. Hence, mass transport instantaneously enhances droplet flow velocity back. This goes on in a repeated, cyclic way. In order to explain this relation mathematically, quite complex computer aided iterative calculations are performed and presented in the Results section.

Convective and Diffusive Mass Transport together; The Mass Transport, is the most important agent in this research. All the other means of transport of matter and energy is used to enhance or keep the mass transport of the species under control within the channels. The concentration has always been the weightiest parameter in all the calculations and considerations.

There are several factors that affect mass transport which are explained by Fick's Law which is in analogy of driving force over the resistance relation. Fick's Law creates the basis of the most models explaining diffusion of substances (Cui, Dykhuizen et al. 2002, Li 2006). **Equation.1** and **equation.2** are solved by Comsol Multiphysics in transport of diluted species module and derived from Fick's Law and continuity equation of conserved quantities to express convection and diffusion together.

$$\textit{Continuity equation:} \quad \frac{\partial \rho}{\partial t} + \nabla \cdot (\rho \mathbf{u}) = 0 \qquad \textbf{(eq.7)}$$

$$\textit{Fick's 1}^{st}\textit{ law:} \quad J = -D\,\frac{\delta C}{\delta x} \qquad \textbf{(eq.8)}$$

$$\textit{Fick's 2}^{nd}\textit{ law:} \quad \frac{\delta C}{\delta t} = D\,\frac{\delta C^2}{\delta x^2} \qquad \textbf{(eq.9)}$$

Where, C: concentration, u: relative velocity, D: diffusion coefficient, t: time, J: Flux, x: distance.

Convective transport is the mass transport mechanism that is maintained by a bulk flow. Existence of velocity difference between fluid flow and a point which emits particles leads to formation of convective mass transport. Diffusive flux is the less dominant component of the mass transport and is maintained by the molecular motions. Diffusive flux always occurs no

matter what material is the media or what physical state the media is in. Physical conditions only affect the rate of the diffusion. Convective mass transport only exists when a fluid flow is presented into the system. Fluid flow can be naturally occurring or may be a forced flow maintained by fans or other equipment. In our system pressure driven forced convection is employed. Diffusive mass transfer also contributes to our system especially within the aqueous droplets.

A global method used to compare convective and diffusive mass transport is validation of Sherwood Number. It is an important measure for comparison. It indicates the ratio of convective diffusion over molecular diffusion and is expressed as:

$$N_{sh} = \frac{k.L}{D}$$
(eq.10)

where, k: convective diffusion coefficient, L: characteristic length in here 'radius of droplet', D: molecular diffusion coefficient.

Mass transport within the droplet and out of the droplet has distinct divergences and they should be handled separately. On **Figure-2.1,** our system is separated into three regions for ease of understanding. Also mobile and immobile phase assumption can be exerted to reduce the complexity of the calculations. Considering the relative positions of the phases with respect to time, water can be addressed as the mobile substance in organic phase surrounding the droplet which is presented as region-I- on **Figure-2.1**. Within the droplet (region-II- and -III- on **figure.2.1**), CPA can be addressed as the mobile substance diffusing through water and cell membrane, but not diffusing into organic phase. The mutual effect of two mass transport actions on each other in two different regions (inner and outer droplet) can be constructed through amount of water present in the droplet. As water migrates from the aqueous droplet surface into the organic phase, water amount in the aqueous droplet decreases continuously. Since definition of concentration is the ratio of mass content to volume of solution, decrease in the solution volume leads to an increase in the concentration.

Mass transport mechanism within the droplet is considered to be molecular diffusion only. Circular flow motions within the cells caused by interfacial frictions at the droplet surface are not considered, since their effect on the total CPA concentration is insignificant. Also, water

diffusion within the droplet is always faster than it is in organic phase (Bajpayee, Edd et al. 2010).

The most important part of intracellular mass transport occurs at the cell membrane. Cell membrane is permeable to water molecules but it creates a resistive wall for CPA to diffuse. Cell membrane is not permeable to most CPA molecules like trehalose. However, glycerol is permeable to mammalian cell membrane (Palasz and Mapletoft 1996). In addition to mass transfer laws, mass transport through an organic membrane is defined by **eq.11** and **eq.12**, proposed by Jacobs M.H. in 1932-1933 and revised by Kedem-Katchalsky (Kedem and Katchalsky 1958).

$$\frac{dN_s}{dt} = P_s . A(C_s^e - C_s^i) \qquad \textbf{(eq.11)}$$

$$\frac{dV_w}{dt} = -L_P . A . R . T(\pi^e - \pi^i) \qquad \textbf{(eq.12)}$$

Equation.11 stands for solute transport across cell membrane and **equation.12** represents water transport through cell membrane, where, Ns is solute amount, Ps is solute permeability (a coefficient specific to membrane), A is area, C is concentration, L_p is hydraulic conductivity (a coefficient specific to membrane), V_w is water volume, R is universal gas constant, T is temperature and π is osmolality. Superscripts e and i indicates extracellular and intracellular respectively.

3. Materials and Methods

3.1 Computing Platform

Hardware

All the computations were run on Hewlett Packard Z420 Workstation with Intel Xeon CPU at 3.20 GHz 8 cores 16 threads processor and 32 GB of random access memory (RAM). NVIDIA Quadro K2000 graphics card was integrated to workstation.

Software

64-Bit Microsoft Windows 7 operating system was used in the workstation. Comsol Multiphysics (Version 4.3) Finite Element Modeling software was used to create two and three dimensional models of the microfluidic system. Mathworks MATLAB (Version 2012b) and Microsoft Excel 2010 was used to support the calculations.

The main calculation software was Comsol Multiphysics. Transport of Diluted Species Module of Comsol is employed for the calculation of mass transfer. Laminar Flow module is employed for the calculations of fluid flow. Moving Mesh module is used to create the effect of shrinkage of aqueous droplets. MATLAB functions which compatibly work with Comsol are created for the detailed determination of fluid flow parameters such as relative velocity. Both MATLAB and Microsoft Excel software were used to create data fit curves from the resulting data which is imported from Comsol. Desired data is correlated by curve fits and definition function of the curve is exported back to Comsol for the sake of controllable and less sophisticated calculation sequence. Thin Diffusion Barrier node under Transport of Diluted Species Module is used to create the impact of cell membrane.

Our ultimate model we created was an 8000 micron long channel with fifteen droplets of 100 micron diameter carrying total three cells, and each droplet separated by 400 micron interval from droplet center to droplet center. Channel cross section was 150x200 microns and cells were 25 micron in diameter (see **figure-3.1**).
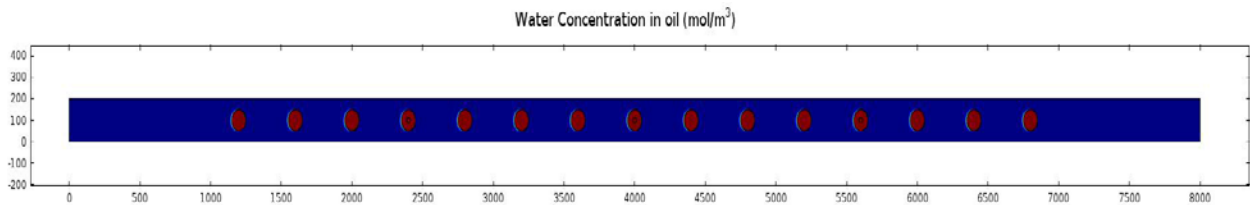
Figure.3.1- Appearance of the system at t=0.

Time dependent solver is used up to 300 seconds. Steps taken by solver were set to free mode, where backwards differentiation formula (BDF) method with maximum and minimum BDF order of 2 and 1 was employed.

Fully Coupled solver type is chosen for the sake of coupling of used physics in the model. Direct linear solver was used as the solver. To be able to conduct Multithreaded Solving (using 8 cores and 16 threads of the processor at the same time for different tasks when possible) Parallel Sparse Direct Solver (PARDISO) was chosen out of three types of Direct Solver. Nested Dissection Multithreaded algorithm is chosen for preordering. Two level scheduling method is chosen, which is a faster method when used with many processor cores. Multithreaded forward and backward solve option is used to improve performance by taking advantage of the processor cores.

Solving method was Newtonian Automatic Highly Nonlinear to achieve high convergence. Smallest allowed damping factor was 1×10^{-9} considering the micrometer dimensions of the system solved with metric system. Newtown Iterations were terminated by tolerance factor which was set to 0.01 with relative tolerance of 0.01.

3.2 Materials

Liquid organic phase was soybean oil which is immiscible with water but has capability of solving water in small amounts (~0.4%) (He, Sun et al. 2004, Bajpayee, Edd et al. 2010). There are several immiscible fatty alcohols that are very capable of solving water. Soybean oil is chosen as the organic phase due to availability and low cost. Investigated favorable organic phases other than soybean oil were given in **appendix-1**. In experiments, surfactant was added to water droplets to render them form droplets easily in organic phase.

Silicon and glass have been used in microfluidic devices in the early periods of development as acts of the influences came from the microelectronics technology applications. Later, polydimethylsiloxane (PDMS) and similar plastics have replaced the use of silicon in microfluidics. Silicon parts are still in use for valves and pumps and other rigid components of the microfluidic system but main structure consists of plastics and polymers today (Jessamine M. K. Ng 2002). Silicon is more expensive and not transparent to ultra-violet or visible light. This downside of silicon prevents use of optical methods of detection over microfluidic devices (Whitesides 2006).

PDMS is an optically transparent soft elastomer with properties completely different than silicon. It supports use of pneumatic valves and provides ease of creation of the structure of microfluidic system. One disadvantage of PDMS is the mechanical or thermal reliability of the material. When necessary, glass, steel or silicon are useful materials to form rigid, thermally and chemically stable components. These materials are also useful in Nano-fluidics technology where channels need to be rigid (Mijatovic, Eijkel et al. 2005). On biological applications usually polymeric structure is preferred for manufacturing of microfluidic devices. They are easy to build by molding and transparent enough to allow use of optical methods of detection. Also PDMS is hydrophobic on surface which is often advantageous for biological applications. The devices we studied are made of PDMS channel patterns bonded on glass slide, which creates three consecutive PDMS side and a glass side for rectangular micro-channels.

The manufacturing process for the polymeric micro-channels starts with visualization of 2-dimensional channel pattern drawn in computer aided design software (in our work AutoCAD). This allows sensitivity through manufacturing process. In order to achieve the nanometer scale sensitivity, surface lithography is employed at the beginning of the process. The pattern drawn on CAD software is transferred on a silicon wafer by surface lithography. After this step, it is possible to produce a mold with the same height as the channel height. Mold is used as the negative replica of the channel pattern and 3-dimensional microchannel production can be started with casting the PDMS solution over the mold. Polymer solution is left to desiccation in a vacuum chamber to remove bubbles formed in the viscous polymer solution. Dried and bubble-free polymer removed from the surface and the mold is taken out.

At this step, three-sided rectangular micro-channel on the surface of PDMS is obtained. Finally, a glass slide is taken and put into oxygen plasma to make surface available to bond for PDMS. Polymer is put on the slide to bond in the way micro-channel will be left between the glass and the polymer. Result is a micro-channel with rectangular cross section available to monitor through glass side (see **Figure.3.2**).
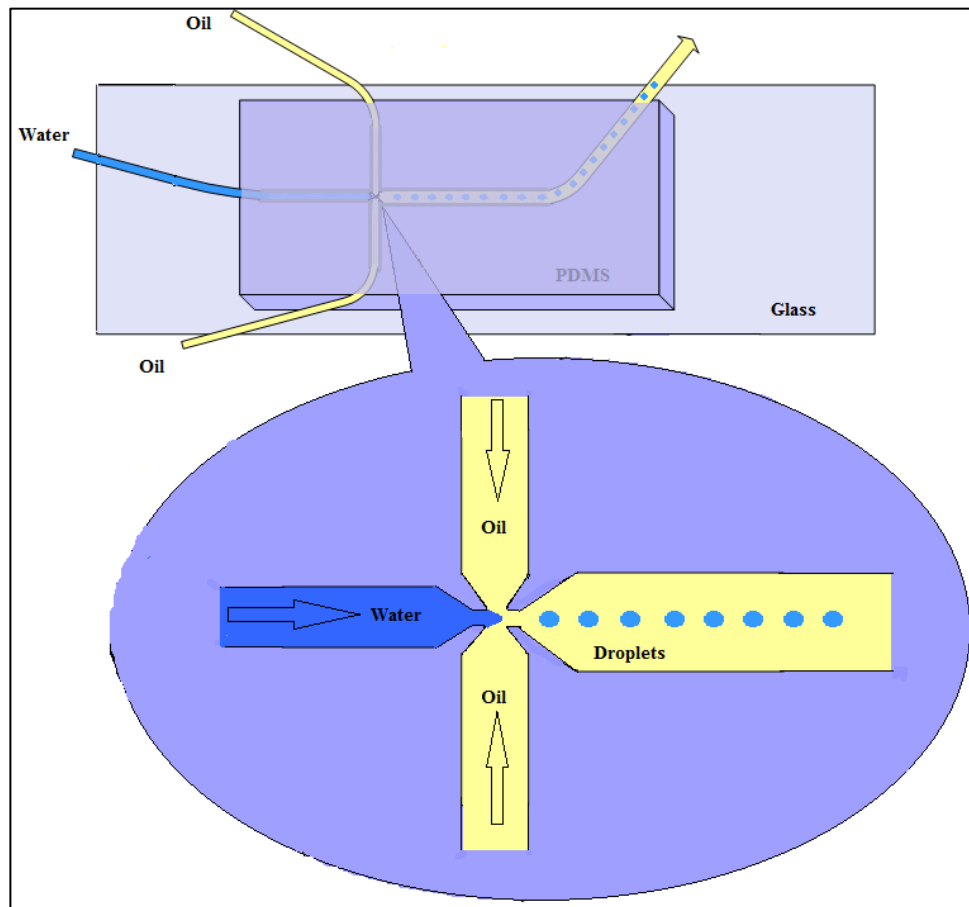

Figure.3.2- Microfluidic channel and the T-junction where droplets are generated.

3.3 Syringe Pump

In order to feed a microfluidic system one must have a very sensitive pumping system like peristaltic pumps or syringe pumps. The one used in the experiments was a syringe pump since it has a better sensitivity and has a flow control software interface through pc. Syringe pumps are systems that simply press a syringe very gently as defined by the user interface. Our pump Nemesys Syringe Pump was capable of pumping three syringes simultaneously and each flow rate can be adjusted separately from nanoliter to milliliter precision. Ends of the

syringes were connected to microfluidic device as feeds. Connection tubings were polymeric tygon tubes made and have inner diameter of around 100 µm (see **figure-3.3**).
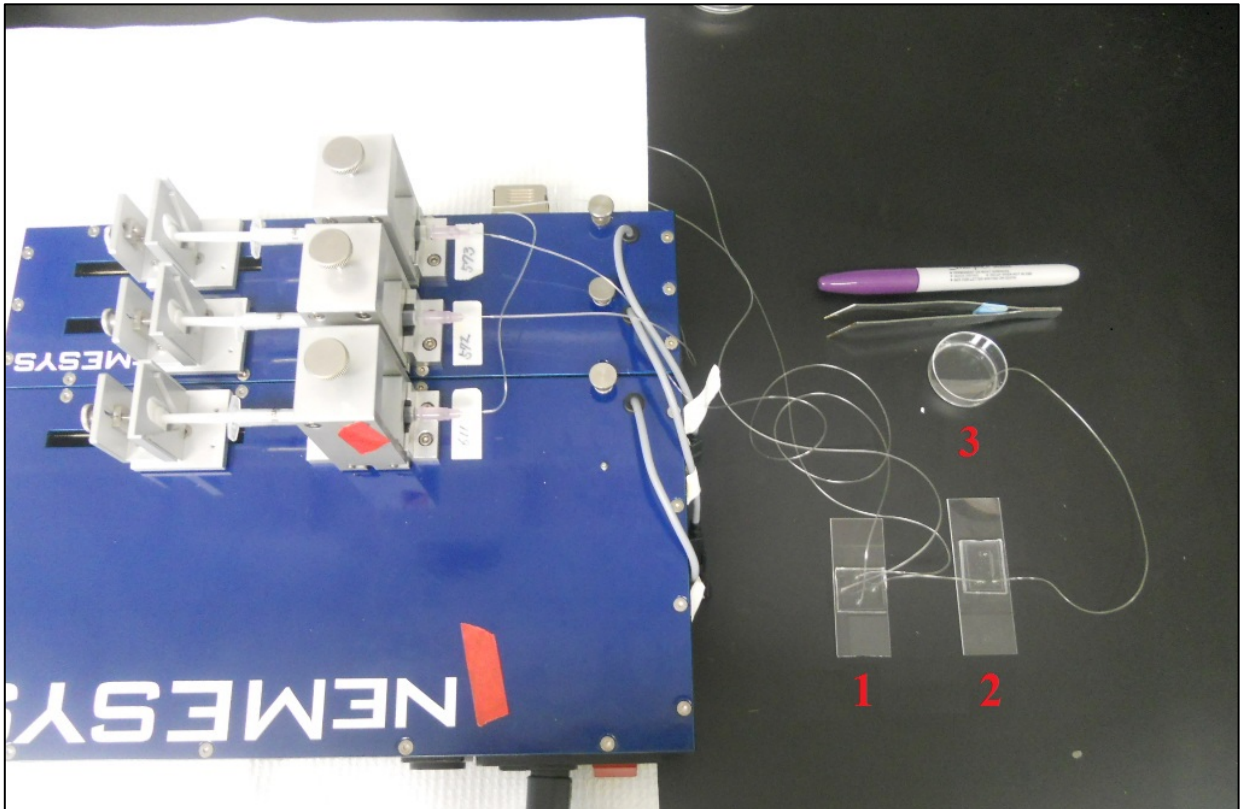
Figure.3.3- Syringe pump and a microfluidic setup developed by S. Onel at the Center for Engineering in Medicine and BioMEMS Resource Center. Numbers indicating order of flow from microfluidic devices to petri dish in the end.

3.4 Inverted microscope

We used an Axio Observer model fluorescent inverted microscope made by Carl Zeiss. It was an inverted microscope allowing us to feed through the PDMS from upside and monitor micro-channels from the underside through glass. Microscope also had a user interface allowing us to observe through computer screen and save or analyze results (see **figure.3.4**). We were able to change flow rate by syringe pump interface and see the effects by microscope interface on the same screen.
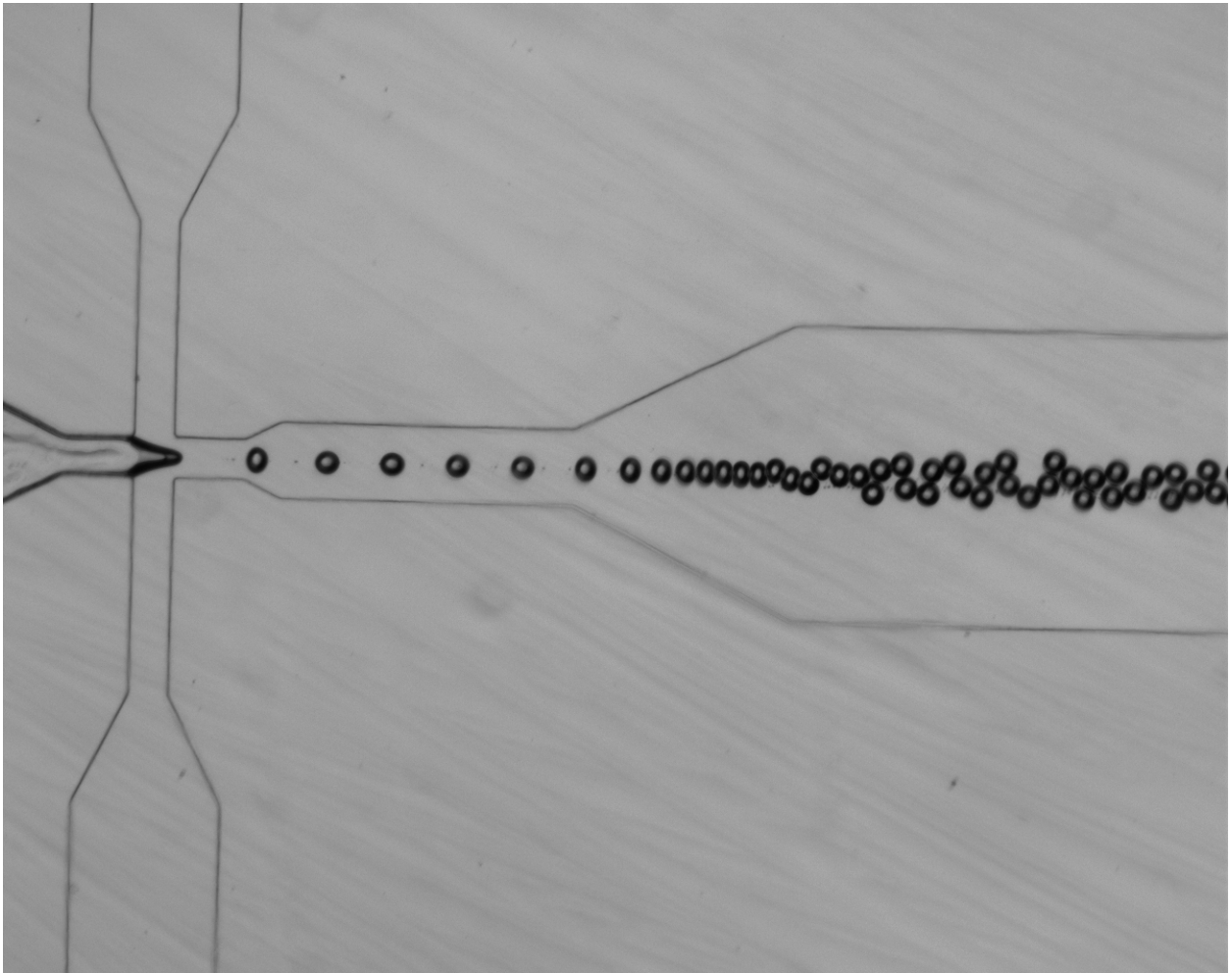
Figure.3.4 – A microscope image of pre-generated droplets. Droplets were generated by a T-junction.

3.5 ITO-Heaters

We used transparent heaters coated with Indium Tin Oxide (ITO) on one side. ITO cover over glass surface allows heating of glass rapidly when an external excitation is applied by DC voltage signals with certain wavelength absorbed by ITO layer. These heaters work with an analog controller system and a thermistor probe, which can maintain temperatures between 0-50 °C. Heater is placed under the microfluidic device to heat through very thin glass without preventing any optical detection.

4. Results and Discussions

4.1 Calculations

4.1.1 Explanation of the Model

Calculation process was conducted in two steps, starting with the solving for concentration and water flux parameters in step-1. This very first stage of calculation is conducted through **eq.1 and eq.2** on Comsol software. Relation between relative velocity and water flux is given in equation 2. In addition to this, relation between aqueous droplet radius and relative velocity is introduced separately via **eq.3 set**. At this point, water flux and relative velocity can be defined as a function of droplet radius, leaving only time dependency of these parameters unknown. The relation given by **eq.13** interprets time dependency relation by closing the circular dependency loop of these three parameters (see **Loop** on **figure 4.1**).

$$\int_{R_i}^{R_0} V_i = \int_{R_i}^{R_0} J_i \cdot A_i \cdot t_i \qquad \textbf{(eq.13)}$$

where, V_i is volume of droplet, J_i is water flux into the organic phase, A_i is area and t_i is time. Noting that subscript i denotes time dependency.

Step-1 is ended by derivation of time and/or position dependent flux, aqueous droplet radius and relative velocity parameters. Results are used to start step-2, where calculations inside aqueous droplet are carried out (Region II and III on **figure-2.1**).

The first parameters used in step-2 are the time dependent droplet volume and shrinkage rate of aqueous droplets which are leading to increase in concentration and are given by,

$$C_{i\_CPA} = C_{0\_CPA} \cdot \left(\frac{V_0}{V_i}\right) \qquad \textbf{(eq.14)}$$

$$\frac{dR_i}{dt} = U_{shrink} \qquad \textbf{(eq.15)}$$

Where, C_{i_CPA} is CPA concentration at any time, C_{0_CPA} is initial CPA concentration and V0 and Vi are initial and time dependent aqueous droplet volume respectively.

Initially 0.5 M CPA is introduced into the droplets. 0.5 M CPA is a concentration value at which some of the mammalian cells can hold vitality up to hours (Karow, Carrier et al. 1968). Then, as the heat is supplied to system, concentration value is increased proportional to ratio of water removal. Concentration values up to 6M are considered in this research, since 6M CPA is the value to achieve vitrification below 100 $^{\circ}$C/s cooling rate (Warkentin, Stanislavskaia et al. 2008). It is needed to increase concentration rapidly in order to avoid toxic injury as much as possible (Fahy 1986).

C_{i_CPA} value is fed into the **eq.16** and **eq.17** as the concentration value C_i. Comsol Multiphysics software uses **equations 16 and 17** when only diffusive flux is employed. These equations are simplified forms of **eq.1** and **eq.2** by the removal of convective terms and they depend on 'D' diffusion coefficient.

$$\frac{dC_i}{dt} = \nabla \cdot (D \cdot \nabla C_i) \qquad\qquad \textbf{(eq.16)}$$

$$J_i = -D \cdot \nabla C_i \qquad\qquad \textbf{(eq.17)}$$

After solving for concentration of CPA in the droplet, **eq.11** was introduced to system for calculation of ultimate result parameter **C$_{intracellular}$**, the concentration of CPA in the cell. The mass transfer module in Comsol needs to be modified to model the diffusion through cell membrane described by **eq.11** which employs permeability coefficient 'P$_s$'. One should convert P$_s$ to D using the **eq.18** derived from **eq.2** and **eq.11**;

$$-D = P_s . \Delta\text{x} \qquad\qquad \textbf{(eq.18)}$$

where, Δx represents the cell membrane thickness, Ps represents membrane permeability and D represents diffusion coefficient.

A flow chart of the aforementioned algorithm is given on **figure 4.1**.

Finally, noting some incidents,

- **Equation.1 and .2,** where terms including 'u' represent contribution of convective mass transport and terms including 'D' represent contribution of molecular transport. In fact,

there is another term referred as the contribution of rate of creation or destruction of substances within the system symbolized by 'R'. However, neither there is such a reaction in our system, nor we need to calculate it. Hence, **equation.1** is actually a simplified form of convection-diffusion equation.

- The fact that the relative flow velocity of droplets is the key feature to calculate convective mass transport. One can see on **equation.1** that flux value is directly proportional to relative velocity which is in fact the dominant factor that affects the flux. Increase in the relative velocity is the main reason for increase in water flux.

- Total volumetric flow rate in the channel was 205 µl/s, which is equivalent of 683 µm/s linear velocity defined as U_{avg}.

- PDMS and glass channel surfaces have very smooth surfaces allowing fluids to flow without forming considerably thick immobile films over the walls. Hence, a slip velocity model has been used in the calculations with ~10 percent of the average velocity and slip length of couple of microns for flow of the organic phase over channel surface.

Values of some parameters used in the calculations are given in table-4.1.

Table-4.1 – Values of parameters referred to literature.

Parameter	Value	Reference
Water diffusion coefficient in Soybean oil (D_{wtr})	$0.5*10^{-10}$ m^2/s	(He, Sun et al. 2004, Bajpayee, Edd et al. 2010)
Glycerol Diffusion coefficient in water	$0.825*10^{-9}$ m^2/s	(Ternström, Sjöstrand et al. 1996)
Cell membrane solute permeability (P_s)	$8*10^{-6}$ m/s (*)	(Yamaji, Valdez et al. 2006, Heo, Lee et al. 2011, Vian and Higgins 2014)
Cell membrane thickness	$8*10^{-9}$ m	(Bruce Alberts 2008)
Viscosity of Soybean Oil (μ)	0.058 kg/m.s	(Tong Wang 2005)

(*****)Value is chosen according to literature. Value may vary depending on type of the cell.

Givens: C_i, C_f, R_0, U_{avg}, ΔP, L, w, μ, D_{wtr}
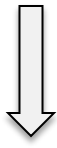
$U_{(i)}(t, R_i(J)), R_i(t, J_i(U))$

COMSOL

$$\frac{dC_i}{dt} = \nabla \cdot (D \cdot \nabla C_i) - u \cdot \nabla C_i$$

$$J_i = -D \cdot \nabla C_i + u \cdot C_i$$

B.C.1 : $x = R_i$, $C = C_f$
B.C.2 : $x = \infty$, $C = C_i$

LOOP

EXCEL or MATLAB

$$\int_{R_i}^{R_0} V_i = \int_{R_i}^{R_0} J_i \cdot A_i \cdot t_i$$

$$U_i = \left(R_i^2 - \frac{w^2}{4} \right) \cdot \frac{\Delta P}{L \cdot \mu \cdot 2}$$
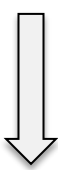
$C_i(t,x)$, $J_i(t,x)$

················· **Step -1-** ·················

$V_i(R_i)$, $A_i(R_i)$
$\Delta V(V_i, V_0)$
$C_{i\_CPA}(t_i, x, C_{0\_CPA})$

Givens: $X_{membrane}$, $V_0(R_0)$, $A_0(R_0)$, C_{0_CPA}, $D_{glycrol}$

COMSOL

$$\frac{dC_i}{dt} = \nabla \cdot (D \cdot \nabla C_i)$$

$$J_i = -D \cdot \nabla C_i$$

$$\frac{dN_s}{dt} = P_s \cdot A \cdot \left(C_s^e - C_s^i \right)$$

$$-D = Ps \cdot \Delta x \ , \ \frac{dR_i}{dt} = U_{shrink}$$

$C_{intracellular}$

················· **Step -2-** ·················

Figure.4.1 – Algorithm generated to solve the system. C_i and C_f are saturated soybean oil concentrations at 20 C and 45 C respectively. R_0 is the initial droplet radius, U_{avg} is the average flow velocity of the organic phase, ΔP is the pressure difference exerted to maintain flow, L is the channel length, w is the channel width, μ is the oil viscosity, D_{wtr} is the diffusion coefficient of water in soybean oil, $X_{membrane}$ is the thickness of the cell membrane, V_0-A_0 are the initial volume and area of the droplet, C_{0_CPA} is the initial CPA concentration in the droplet, $D_{glycerol}$ is the diffusivity of glycerol in water and P_s is the solute permeability of cell membrane. u is the relative velocity between oil and droplet, U_i is the velocity of the aqueous droplets, R is the droplet radius, C is concentration, J is flux, N is mass, t is time, x is distance. Calculations of step-1 with the Loop represents calculations for outer droplet, calculations of step-2 represent the inner droplet. Subscripts 'i' denotes time dependent (anytime), '0' denotes initial, 's' denotes solute, 'shrink' denotes shrinkage. Superscripts 'e' denotes extracellular, 'i' denotes intracellular. $C_{intracellular}$ is the ultimate result of the calculations which represents CPA concentration within the cell at any time.

4.2   Two Phase Flow in Micro-channel / Design Matters

Before going into deeper into details of calculations, some design matters caused by two phase flow must be explained. A flow velocity profile and the position of droplet in the profile were given on **figure-2.6**. That is the conventional laminar flow profile appearance for any Newtonian fluid flowing up to N_{RE} value of 2000. The unconventional outcome of that profile is appears when looked into the average velocity. No matter what velocity the fluid is flowing, the position on y-coordinate where the fluid hits the average velocity is the same (position of the orange line in y-direction on **figure-2.6**). The y-coordinate value, where the fluid flows at the speed equal to the average velocity does not change. This average velocity region, so entitled $R_{critical}$ region, is only a factor of channel width, not flow rate. The importance of such critical value comes up when calculations with average organic velocity is performed. In order to calculate convective mass transfer one must use the average flow velocity of the mobile phase (see **eq.2**). The relative velocity value of our system hits to zero at that critical point, resulting a lower peak of flux magnitude of water into organic phase (see **figure.4.2**).

Change in the radius causes change in relative aqueous droplet velocity which affects flux magnitude as seen in **figure-4.2**. Flux value is lowest at R~=45 and is valid for all flow rates since the $R_{critical}$ value is only proportional to channel width. The proportionality value can be found on slope of **figure-4.3.**
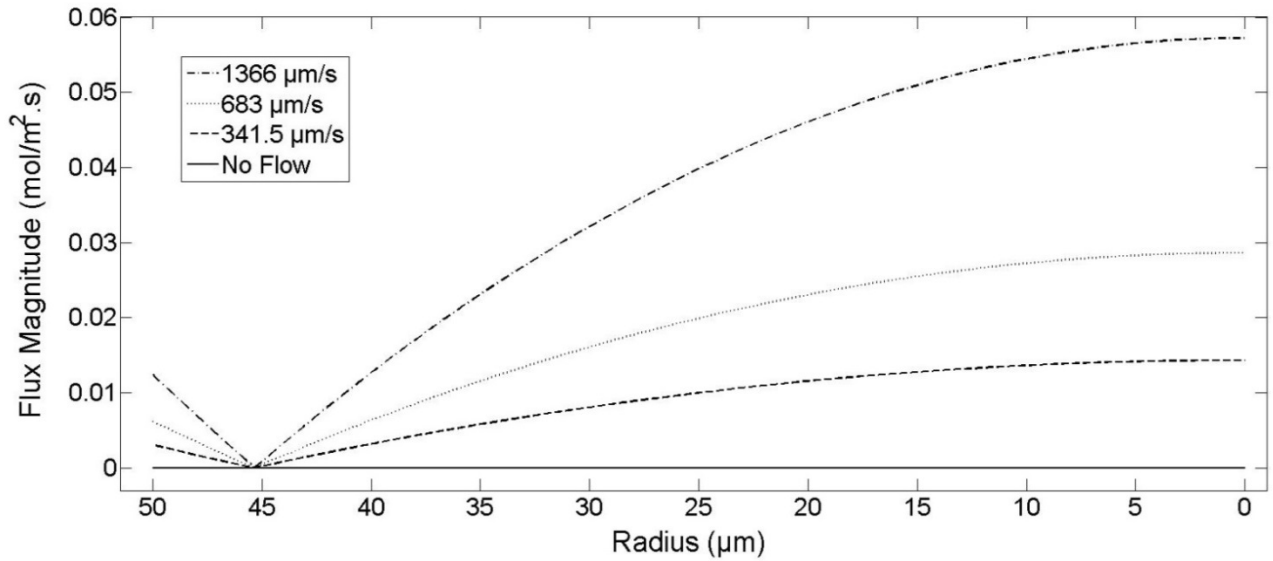
Figure-4.2. Change of flux magnitude with respect to droplet radius for various average organic phase flow rates.

Below R$_{critical}$ value, as the droplet radius decreases flux continue to increase due to increase in relative velocity of aqueous droplets. This increment is proportional to the flow velocity magnitude of the organic phase.

At Rcritical, where relative droplet flow velocity is close to or equal to zero, no convective flow is utilized and a decreased droplet shrinkage rate is achieved. Flux magnitude hits the minimum value which roughly is equal to diffusive flux magnitude.

Figure-4.3 shows the Rcritical values that should be avoided at various channel width values. For example; if droplet size is 150 micron (R =75 micron), one should choose channel width of 250 microns or higher to avoid R critical region. In our research, channel width was 150 microns at minimum and cross-section was 150x200 microns. Hence, R~=45µm region is referred as Rcritical region.
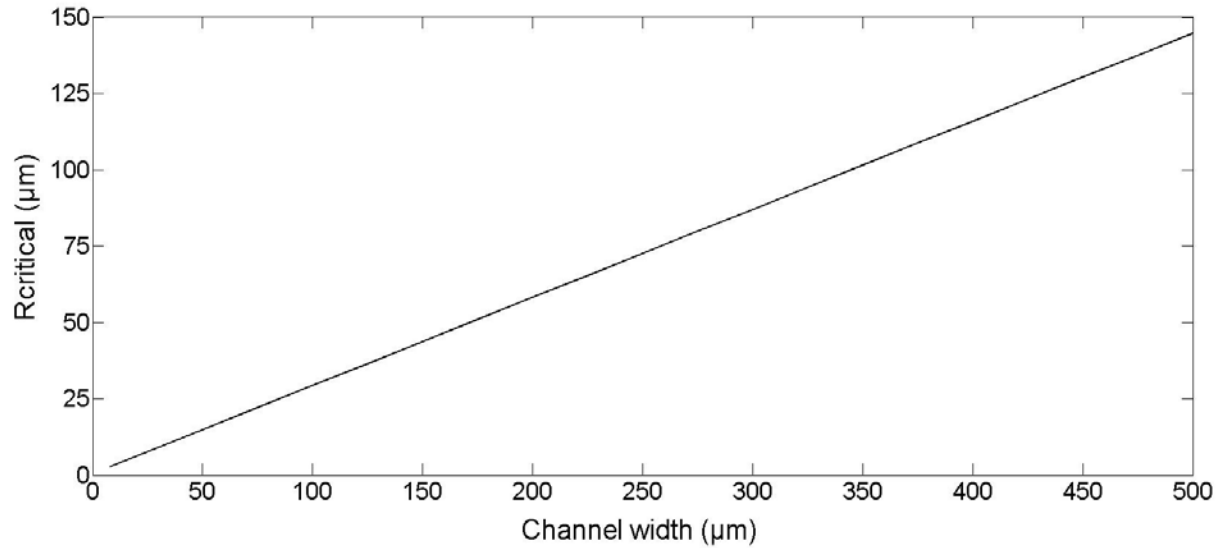
Figure-4.3. Critical Radius value for various channel width values. Equation of the line is **y=0.3028x**.

4.3   Water Transport from Aqueous Droplet to Organic Phase

In this section, calculations mostly related to mass transfer of water into the organic phase are presented. Presented figures are outcomes of the calculations performed on step-1 in **figure 4.1**.

In **figure-4.4** zero flow rate represents the case where only diffusive mass transport takes place. In any magnitude of flow rate > 0, convective and diffusive mass transports take place together simultaneously. Higher relative velocity creates a bigger convective mass transport potential. Droplets shrink the fastest at highest flow rate.
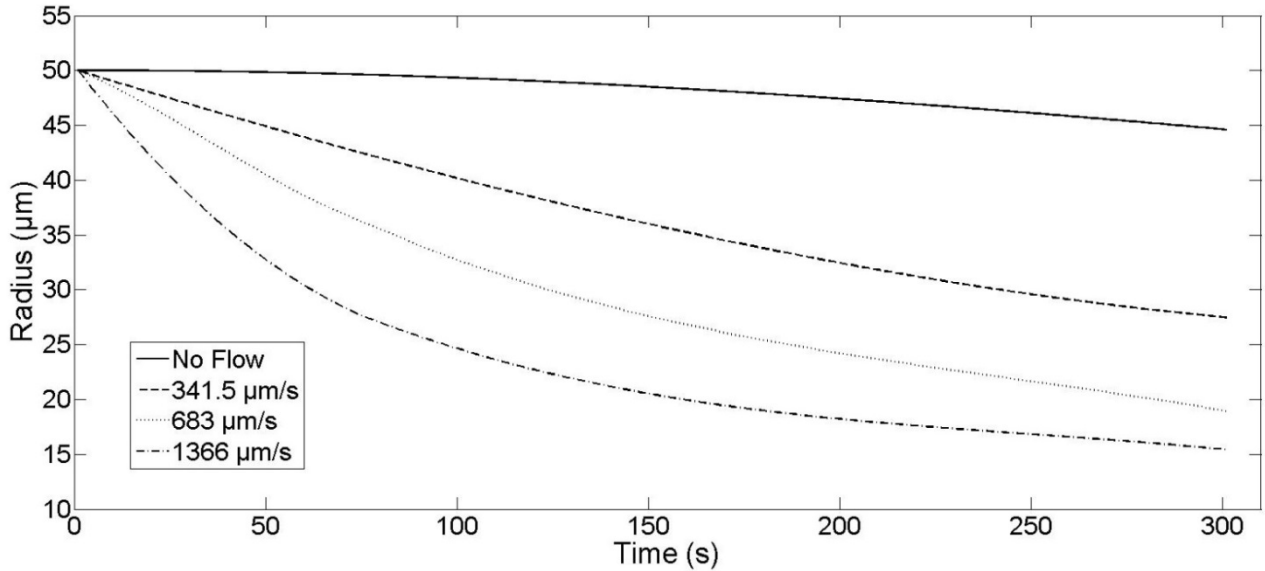
Figure-4.4. Radius of aqueous droplet with respect to time at various flow rates.

Figure-4.5 shows the aqueous droplet velocity relative to average organic phase flow velocity. The points, where relative velocity value is zero, represent the state where droplets are flowing at average bulk phase velocity. This state occurs at the instant, when droplets reach the critical radius at R=45µm. When relative velocity is zero, convective mass transport is at the minimum value (see. **Eq.1 and eq.2**). The relative velocity is analyzed since it is the dominant factor that effects convective diffusion.
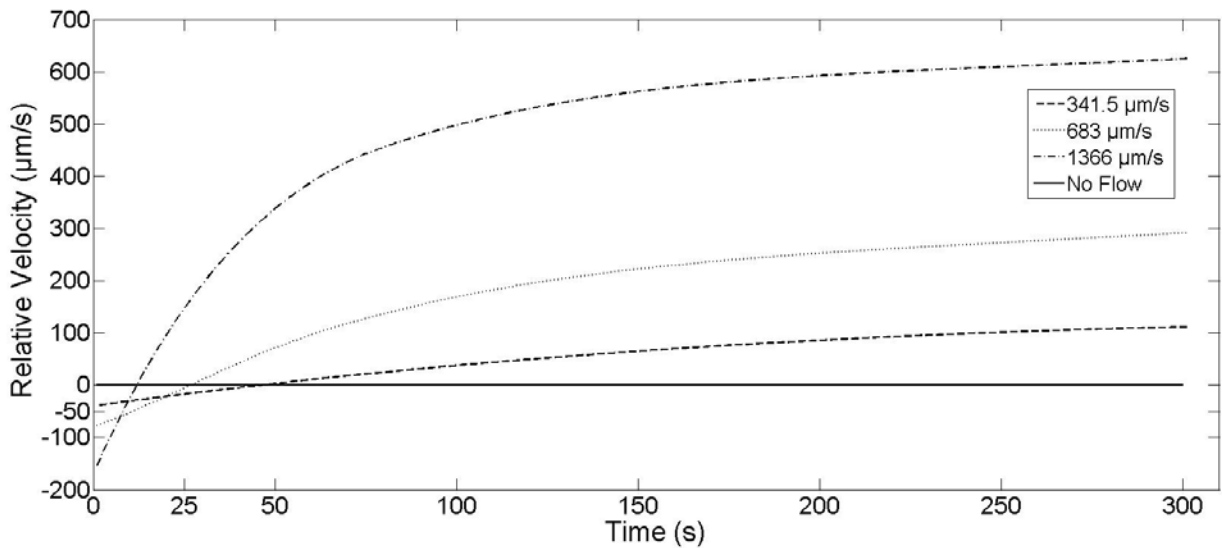
Figure-4.5. Difference between the velocity of aqueous droplets and average organic phase velocity with respect to time.

Figure-4.6 shows the total flux magnitude of water transport from droplet to organic phase. Total flux magnitude is the sum of convective flux magnitude and diffusive flux magnitude. At the instant droplet velocity catches average bulk flow velocity (zero relative velocity), flux values hit a lower peak point, where the flux value is nearly equal to the diffusive flux magnitude or nearly equal to the flux magnitude of No Flow case. Increasing the flow rate causes to achieve higher water mass flux from water to organic phase.
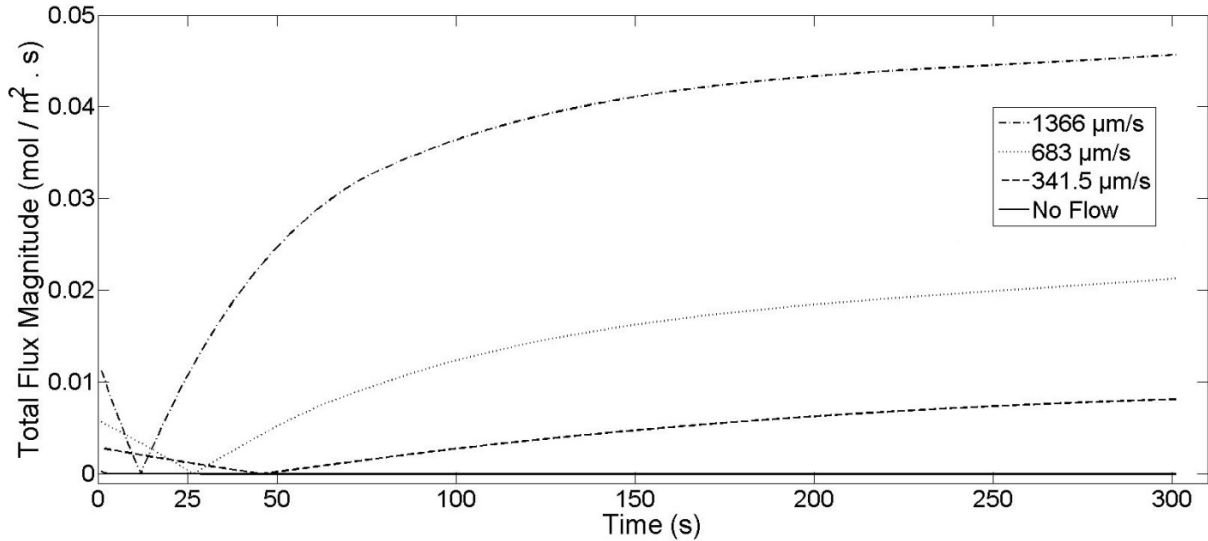
Figure-4.6. Total flux magnitude with respect to time at various flow rates.

Figure-4.6 shows that the flux magnitude is always increasing with time. Surface area of the droplet, where the mass transfer takes place, decreases in time. Hence a decrease in the mass transfer rate occurs when decrease in the area become dominant. **Figure-4.7** is proportional to the multiplication of the results shown in **figure-4.4** and **figure-4.6.** In **Figure-4.7**, 1366 µm/s flow rate line is already at its maximum rate, while 341.5 µm/s flow rate is at the lowest. This indicates the importance of the flow rate for decreasing effects of $R_{critical}$ region and increasing convective mass transfer.
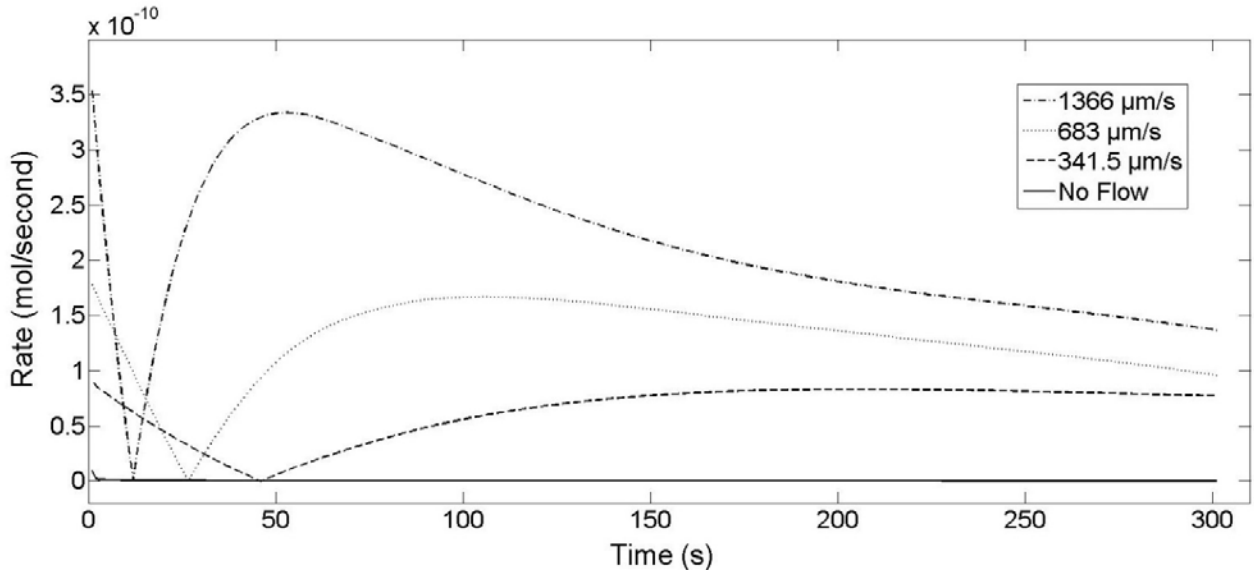
Figure-4.7. Transfer rate of water into organic phase with respect to time.

Figure set-4.8 describes concentration of water in the organic phase at t=30s, 60s, 90s, 120s for various flows. All the profiles of water concentration remain within region-I- on **figure-2.1.** Linear parts of the lines represent concentration of water in the aqueous droplet, where water concentration always defined at the maximum value (saturated water concentration in oil at 45°C). As expected, higher flow rates provide better diffusion of water into the oil compared to the 'No flow', where the flux value is the lowest. 341 µm/s flow rate concentration data stay close to No Flow condition up to 120s. That is a result of low relative droplet velocity values around the Rcritical region. Change in the direction of relative velocity retards the removal of water from the aqueous droplet.
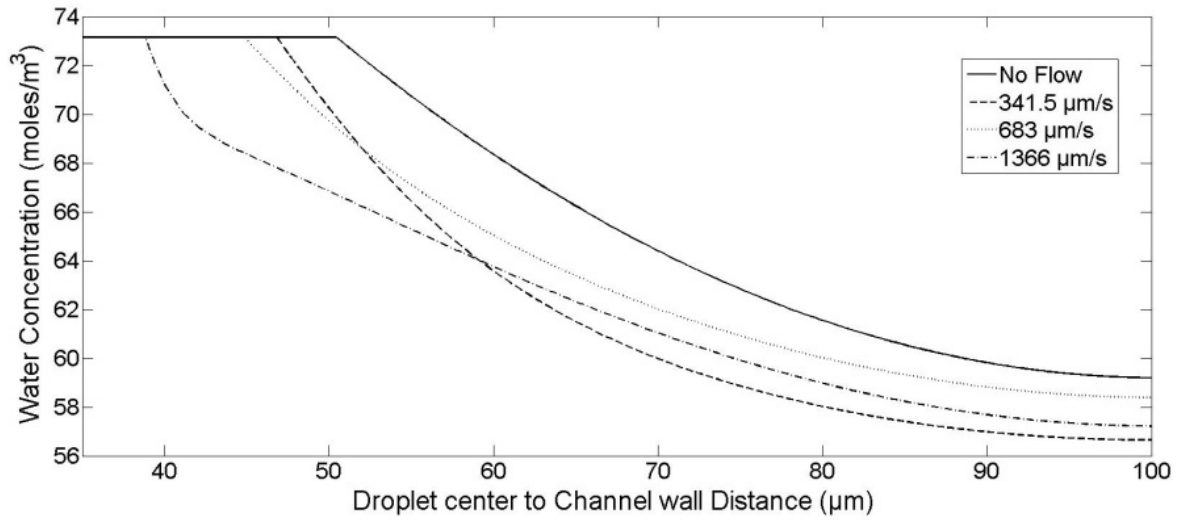
Figure-4.8A. Concentration profiles of water in the organic phase for various flow rates with respect to position between droplet and channel wall <u>at t=30s.</u>
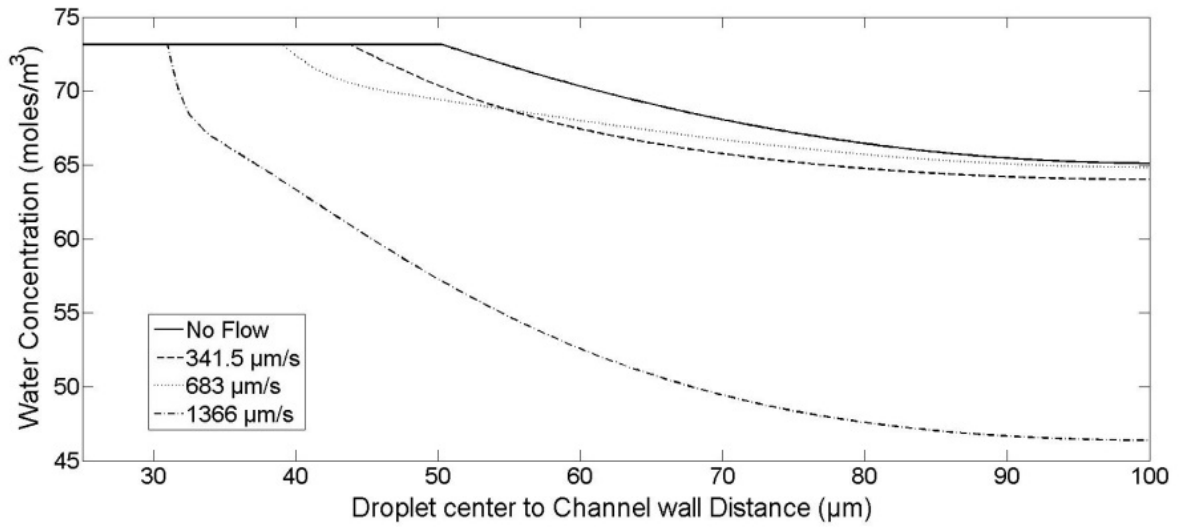
Figure-4.8B. Concentration profiles of water in the organic phase for various flow rates with respect to position between droplet and channel wall <u>at t=60s.</u>
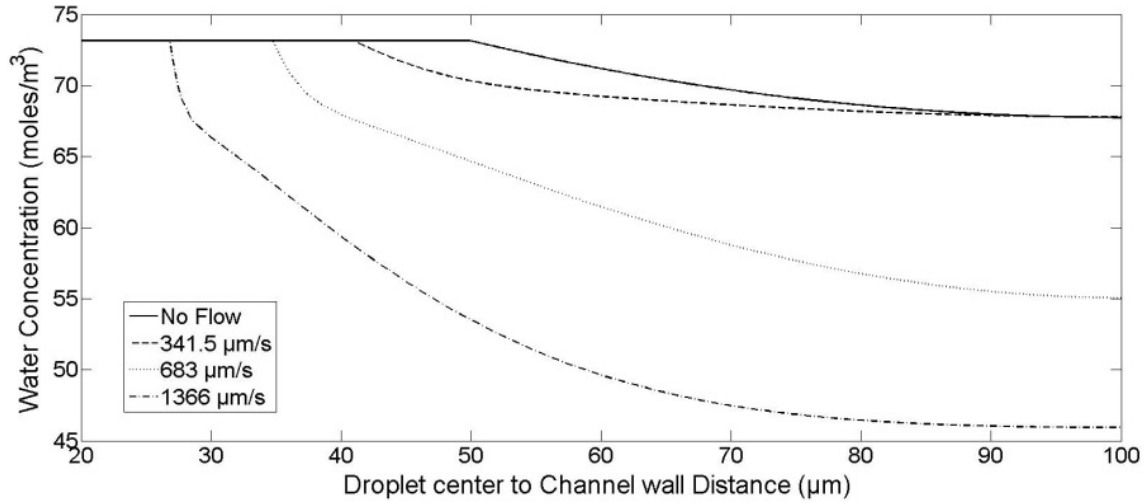
Figure-4.8C. Concentration profiles of water in the organic phase for various flow rates with respect to position between droplet and channel wall <u>at t=90s.</u>
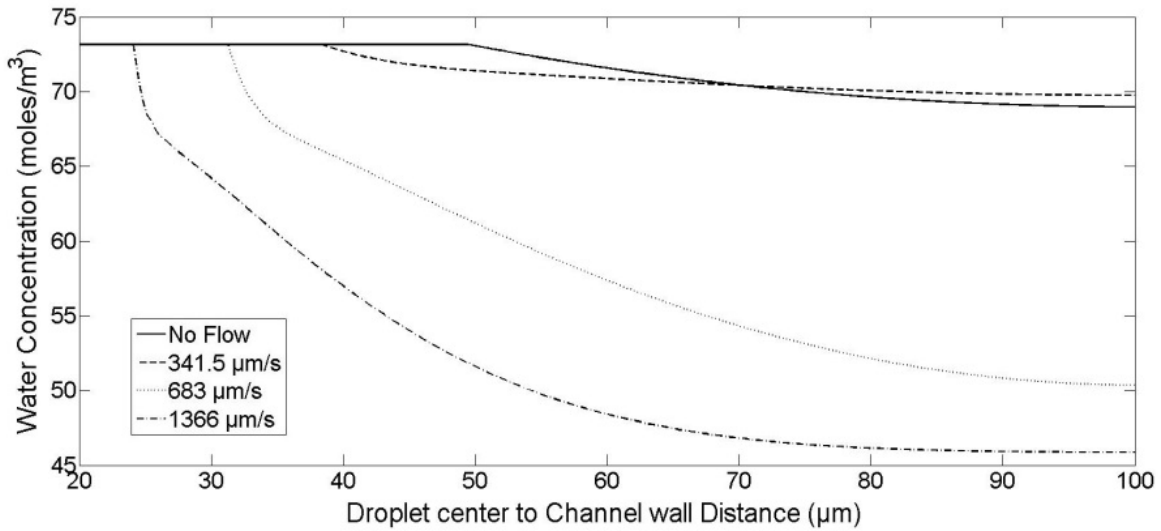
Figure-4.8D. Concentration profiles of water in the organic phase for various flow rates with respect to position between droplet and channel wall at <u>t=120s.</u>

Figure-4.8D shows that 341µm/s flow line reaches R critical region the latest and it stays in that region longer than higher flow rates, due to the lowest shrinkage rate of the droplet at 341 µm/s. Convective diffusion is not sufficient for the 341 µm/s flow rate. Hence a concentration profile close to 'No flow' condition is achieved at the times droplet radius is around Rcritical

region (R~=45microns). After t=120s, droplets in 341µm/s flow rate manage to set a less complicated flow regime and more predictable concentration profile (see **figure-4.9**). This reduced flux occasion is valid for all flow rates (1366µm/s flow line on **figure-4.8A** and 683µm/s line on **figure-4.8B**) but faster the flow rate shorter the time spent in the retarded flow region.

Figure-19 is an image matrix describing water concentration in organic phase for different flow rates at times ranging from 0 s to 300 s. Concentration profiles at high flow rates are more steady than lower flow rates. During the shrinkage of the droplets, when they pass through $R_{critical}$ region, practically a mixing occurs in the channel. During the process, flow direction does not change, but relative flow direction does change. At 341µm/s flow rate and at t=30, average organic phase velocity is faster than that of the droplet velocity. At t~=50 s, droplet radius value is equal to $R_{critical}$ value and the flow rate of droplet and average organic phase is equal. At t=60 s, droplets are shrunk and flow faster than average organic phase flow velocity. Water molecules dragged away from one droplet is now dragging back to the same droplet causing an affect same to mixing instead of dragging away. As a result of low concentration gradient the water mass transport to organic phase slows down. At t=120 s, all the water molecules are dragged far away and a concentration profile of a conventional two phase flow is formed and continued steadily. At 683 and 1366 µm/s flow rates, droplets have already shrunk enough to flow faster than average organic phase velocity at t=30 s. The main advantage of faster flow rates is that the droplets come into contact with higher amounts of fresh organic phase that is less concentrated with water and has better capability of carrying away water molecules. Higher droplet velocity relative to average organic phase yields better mass flux.
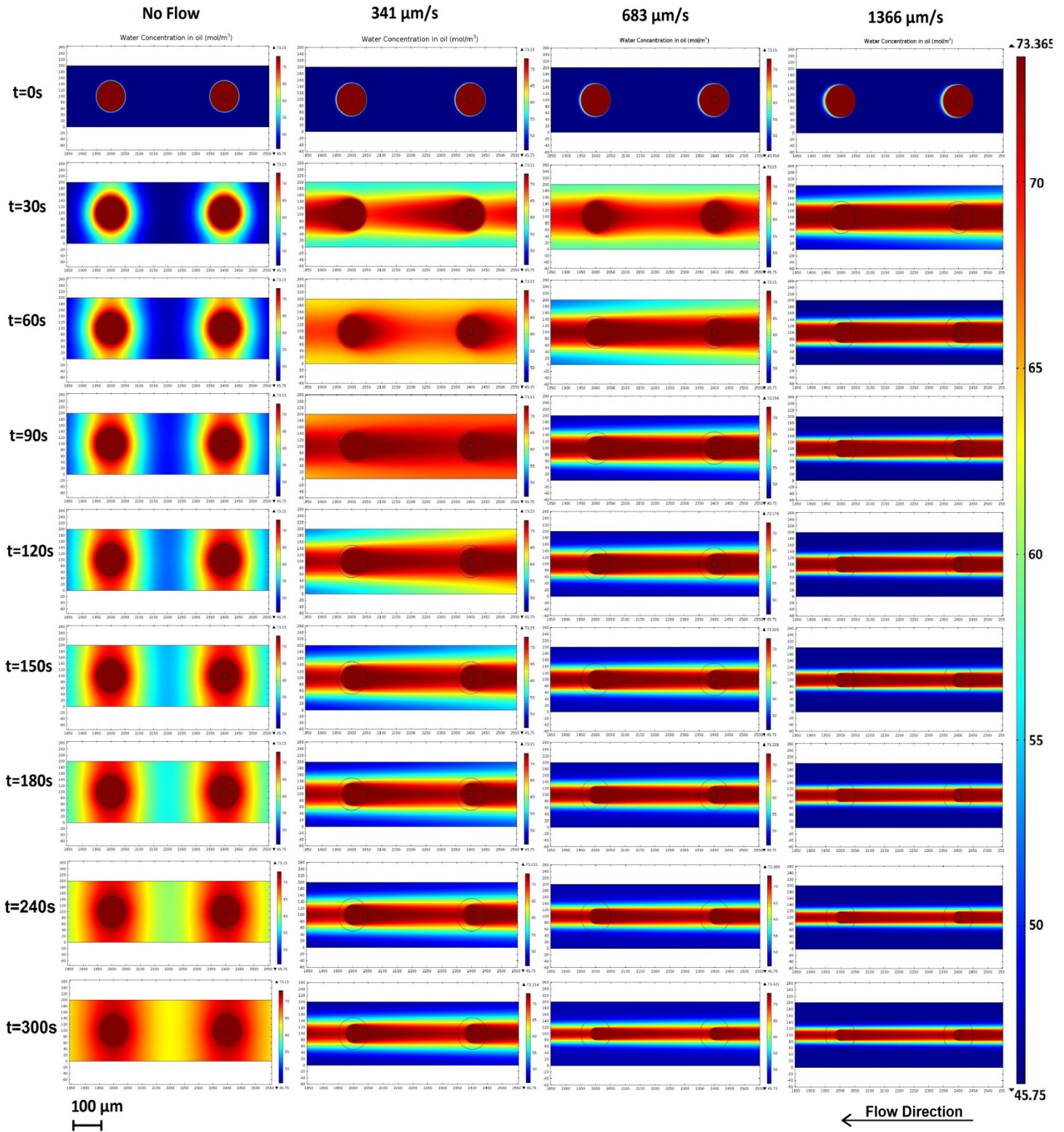
Figure-4.9. Concentration of water (mol/m^3) in organic phase for various flow rates at various times. Initial droplet diameter is 100 microns and channel width is 200 microns.

## 4.4 CPA Concentration Profile within Droplet
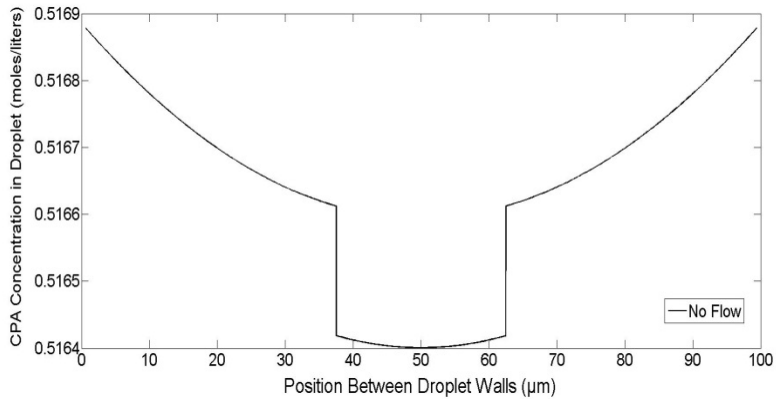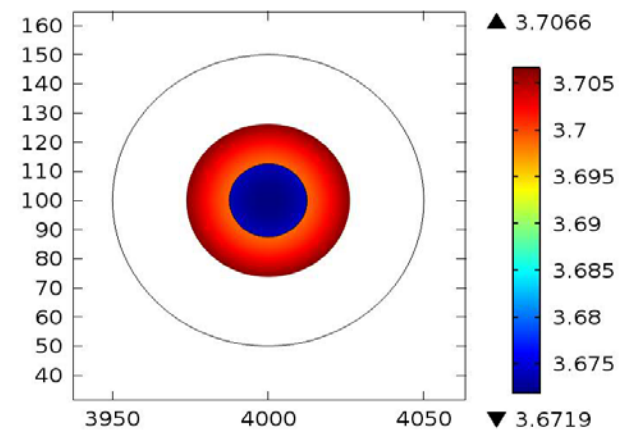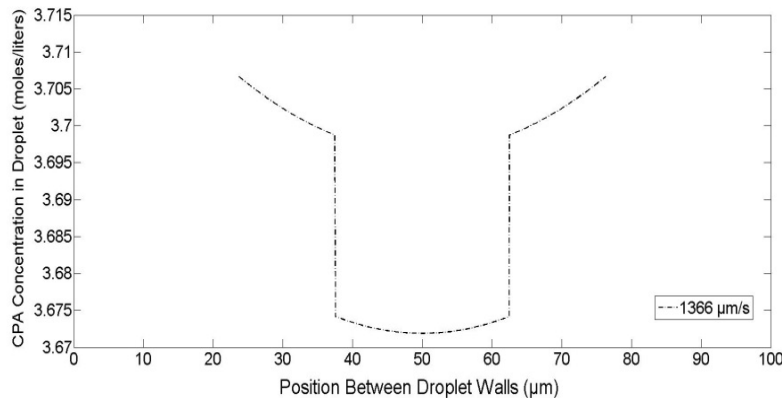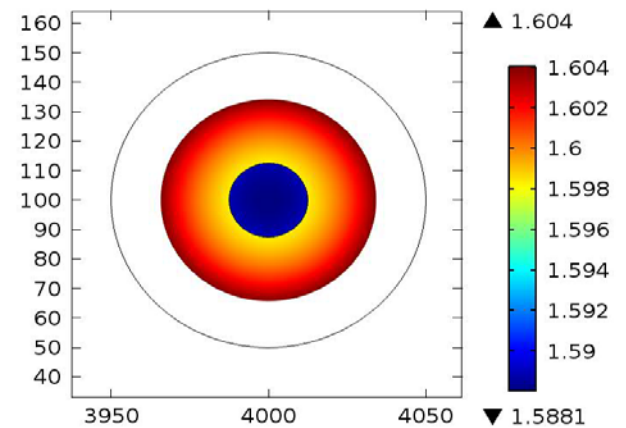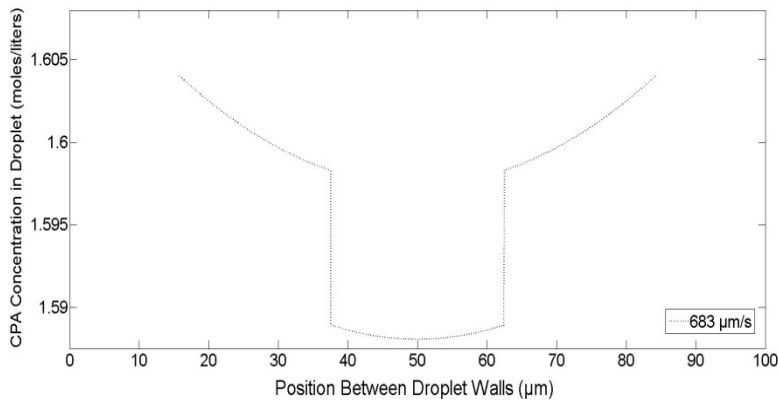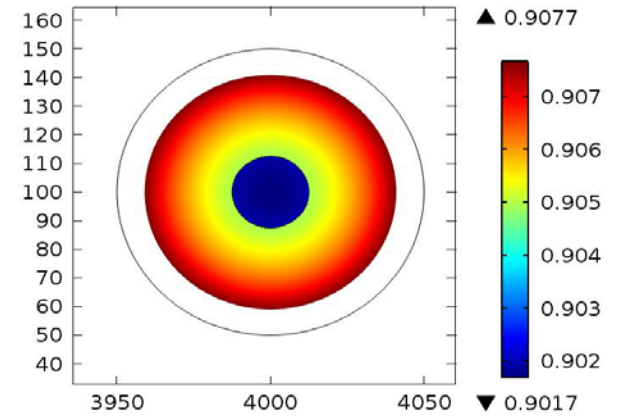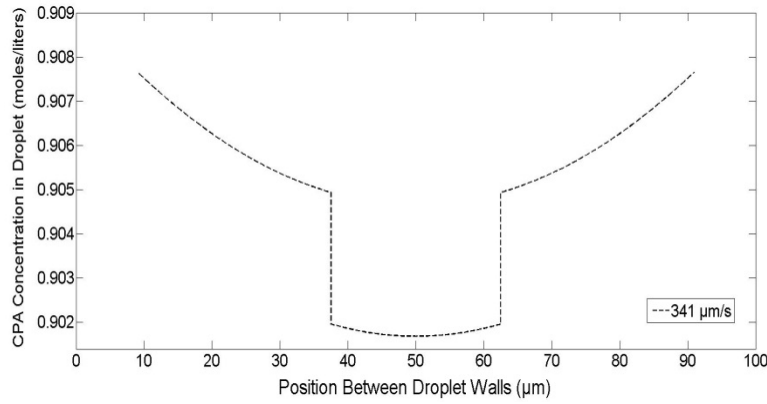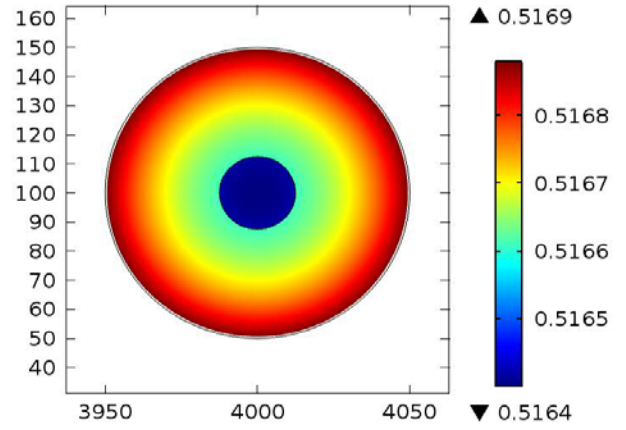
**Figure.4.10 -** CPA concentrations within the droplet for various flow rates at t=90s. All concentrations are in mol/liter. Initial concentration is 0.5M.

Figure-4.10 represents region-II- and -III- shown on **figure-2.1**. Concentration within the droplet is highest at droplet walls since the loss of water takes place at droplet walls in contact with the organic phase. Sudden decrease in CPA concentration is due to resistance of cell membrane against diffusion. Permeability of the cell membrane is used as Ps=8*10^{-6} m/s.
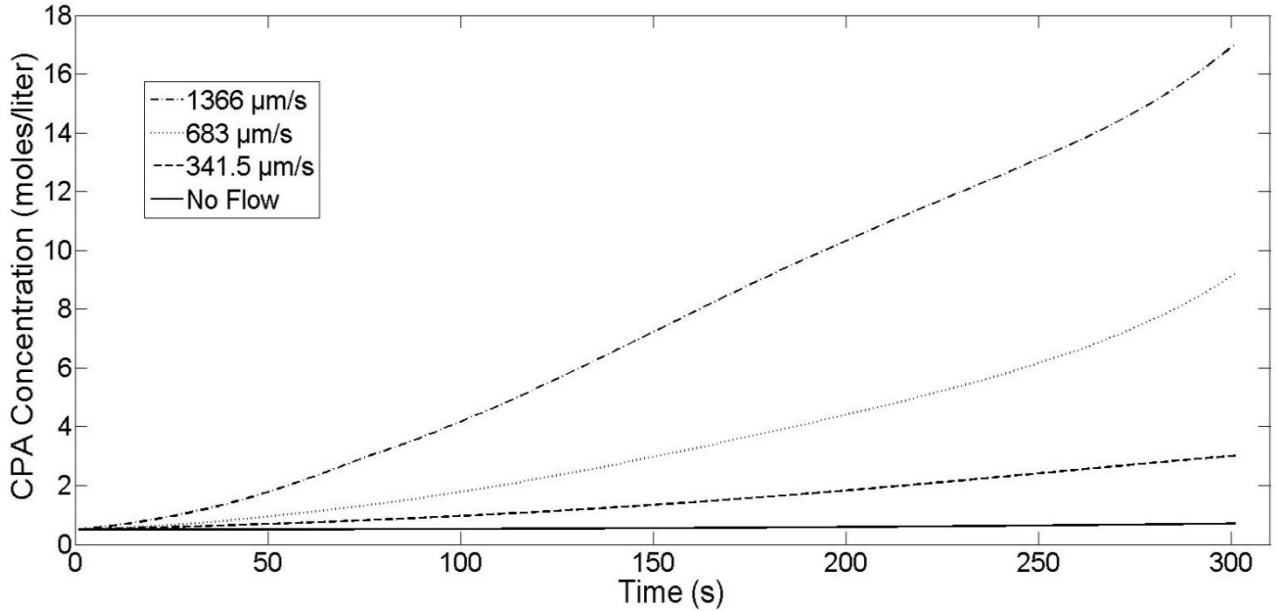

Figure-4.11. Change of CPA concentration within aqueous droplet due to shrinkage at various flow rates with respect to time. Initial CPA concentration is 0.5M.

As higher amounts of water is transported to organic phase with time, less amount of water is remained within the aqueous droplet increasing the concentration of CPA in the droplet as shown in **figure-4.11**. Faster shrinkage rate is achieved at higher flow rates yielding higher CPA concentration values.

4.5 Comparison of Convective and Conductive Water Transport in the Channel

Figure-4.12 indicates the dominance of convective diffusion over molecular diffusion at any flow rate. At R critical, where velocity difference between droplet and average oil velocity is zero Sherwood number peaks to lowest point. Sherwood number is given by **eq.10**.
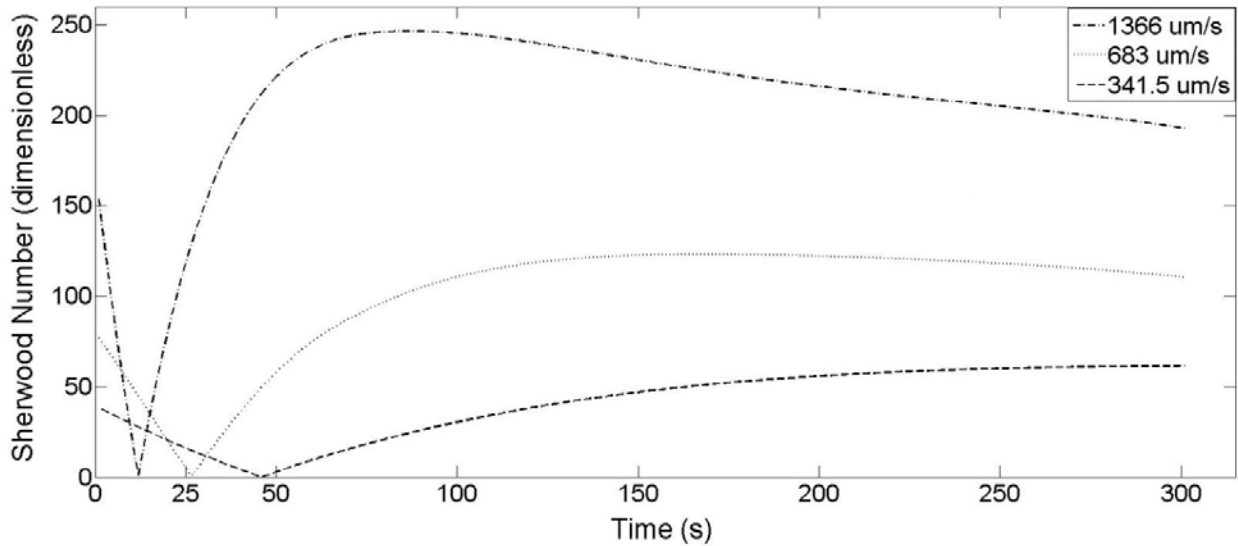
Figure-4.12. Sherwood Number for comparison of convective and diffusive flux at various flow rates.

4.6   Optimization of the Results

Figure-4.13 clearly shows an optimum rate interval for values of droplet radius between R=40µm and R=20 µm. In this interval, the rate of transfer of water into the organic phase is at maximum. If pre-concentration process is operated with 85 micron droplets, a faster increase in the CPA concentration can be achieved. Also Rcritical region will be avoided.
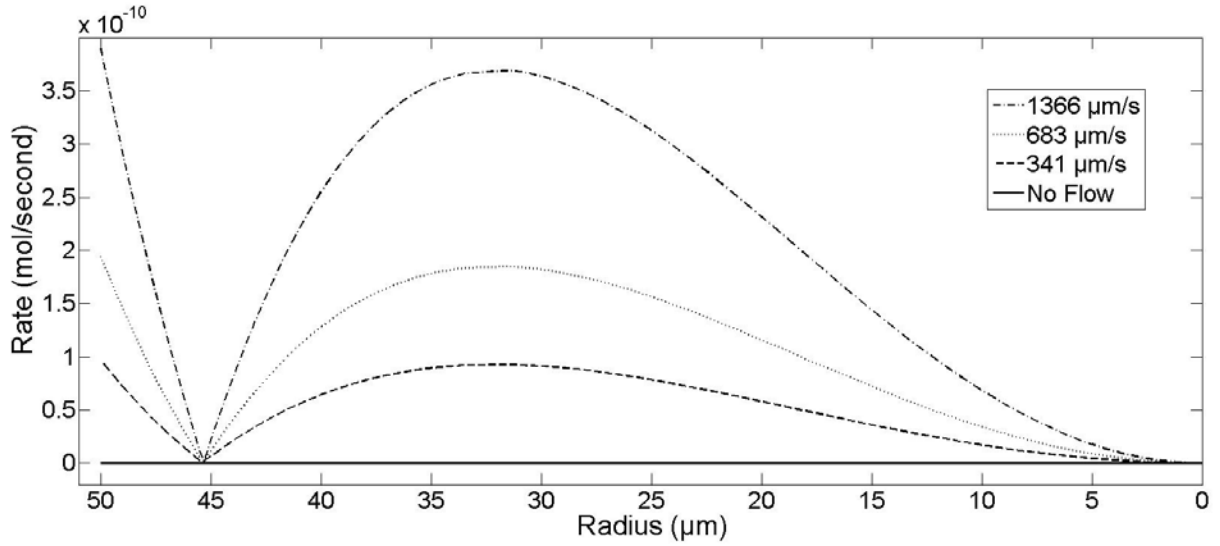
Figure-4.13. The rate of water transfer to organic phase with respect to droplet radius.

It is shown on **Figure-4.4** that it only takes 140 seconds to reduce droplet radius from 42.5 to 20 at 1366µm/s flow rate. That is enough reduction to achieve 9.5 times the initial CPA concentration. If 683µm/s flow rate is applied, it would take 240 seconds to achieve the same pre-concentration rate. **Figure-4.14** summarizes the time needed to achieve certain CPA concentration if starting droplet radius is chosen 42.5µ.
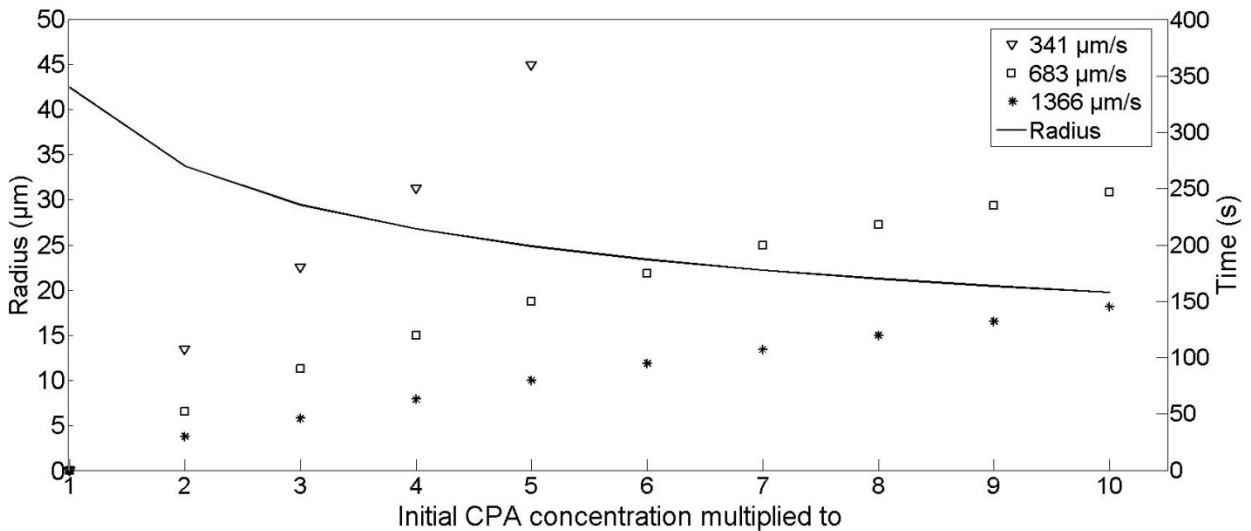
Figure-4.14. Time required to reach multiplies of initial CPA concentration for 85 micron initial droplet size (R=42.5 µm).

With regard of **figure-4.14**, it can be said that at 683 µm/s and 1366 µm/s flow rates it is possible to pre-concentrate cells with CPA in less than 300 seconds. If possible, the flow rate can be increased as needed to achieve faster pre-concentration. Higher flow rate of organic phase is always yielding higher CPA concentrations within droplets while decreasing process time. If one needs to work with highly sensitive cells, they can choose lower initial concentration of CPA concentration to prevent CPA toxicity on the cell while increasing the flow rate as much as possible.

5. Conclusions

- Increasing the average organic phase flow rate enhances the mass transfer rate from droplet to organic phase.

- In order to achieve maximized pre-concentration with droplets, Critical Radius value should be avoided by choosing appropriate channel width. If channel width is 150 microns in the narrowest point, ideally, droplets smaller than 90 micron should be generated.

- Soybean oil is a non-toxic and low cost organic phase, but water solubility of soybean oil is very limited. Fatty alcohols having 8 carbons to 12 carbons in their chains are capable of solving water up to 5% w/w. Those substances should be examined for use in pre-concentration of cells via aqueous droplets.

6. References

Acker, J. P. (2007). "Biopreservation of Cells and Engineered Tissues." **103**: 157-187.

Bajpayee, A., et al. (2010). "Concentration of glycerol in aqueous microdroplets by selective removal of water." <u>Anal Chem</u> **82**(4): 1288-1291.

Beebe, D. J., et al. (2002). "Physics and applications of microfluidics in biology." <u>Annu Rev Biomed Eng</u> **4**: 261-286.

Bruce Alberts, A. J. (2008). <u>Molecular Biology of the Cell</u>, Garland Science.

Chiu, D. T. (2007). Aqueous Droplets as Single-Molecule Reaction Containers. <u>The 14th International Conference on Solid-State Sensors, Actuators and Microsystems</u>. Lyon, France, Transducers & Eurosensors.

Chiu, D. T. and R. M. Lorenz (2009). "Chemistry and biology in femtoliter and picoliter volume droplets." <u>Acc Chem Res</u> **42**(5): 649-658.

Chiu, D. T., et al. (2009). "Droplets for ultrasmall-volume analysis." <u>Anal Chem</u> **81**(13): 5111-5118.

Cui, Z. F., et al. (2002). "Modeling of cryopreservation of engineered tissues with one-dimensional geometry." <u>Biotechnol Prog</u> **18**(2): 354-361.

Czaplewski, D. A., et al. (2003). "Nanofluidic channels with elliptical cross sections formed using a nonlithographic process." <u>Applied Physics Letters</u> **83**(23): 4836.

Dittrich, P. S. and A. Manz (2006). "Lab-on-a-chip: microfluidics in drug discovery." <u>Nat Rev Drug Discov</u> **5**(3): 210-218.

Elmoazzen, H. Y., et al. (2009). "Osmotic transport across cell membranes in nondilute solutions: a new nondilute solute transport equation." <u>Biophys J</u> **96**(7): 2559-2571.

Elvira, K. S., et al. (2013). "The past, present and potential for microfluidic reactor technology in chemical synthesis." <u>Nat Chem</u> **5**(11): 905-915.

Eroglu, A., et al. (2000). "Intracellular trehalose improves the survival of cryopreserved mammalian cells." <u>Nat Biotechnol</u> **18**(2): 163-167.

Fahy, G. M. (1986). "The relevance of cryoprotectant "toxicity" to cryobiology." <u>Cryobiology</u> **23**(1): 1-13.

Hammerstedt, R. H., et al. (1990). "Cryopreservation of Mammalian Sperm - What We Ask Them to Survive." <u>Journal of Andrology</u> **11**(1): 73-88.

He, M., et al. (2005). "Selective encapsulation of single cells and subcellular organelles into picoliter- and femtoliter-volume droplets." <u>Anal Chem</u> **77**(6): 1539-1544.

He, M., et al. (2004). "Concentrating solutes and nanoparticles within individual aqueous microdroplets." <u>Anal Chem</u> **76**(5): 1222-1227.

Heo, Y. S., et al. (2011). "Controlled loading of cryoprotectants (CPAs) to oocyte with linear and complex CPA profiles on a microfluidic platform." <u>Lab Chip</u> **11**(20): 3530-3537.

Ho, C.-T., et al. (2006). "Rapid heterogeneous liver-cell on-chip patterning via the enhanced field-induced dielectrophoresis trap." <u>Lab Chip</u> **6**(6): 724-734.

Janasek, D., et al. (2006). "Scaling and the design of miniaturized chemical-analysis systems." <u>Nature</u> **442**(7101): 374-380.

Jeffries, G. D., et al. (2007). "Controlled shrinkage and re-expansion of a single aqueous droplet inside an optical vortex trap." <u>J Phys Chem B</u> **111**(11): 2806-2812.

Jeffries, G. D., et al. (2007). "Dynamic modulation of chemical concentration in an aqueous droplet." <u>Angew Chem Int Ed Engl</u> **46**(8): 1326-1328.

Jessamine M. K. Ng, I. G., Abraham D. Stroock, George M. Whitesides (2002). "Components for integrated poly(dimethylsiloxane) microfluidic systems." <u>Electrophoresis</u> **23**: 3461–3473.

Karow, A. M., et al. (1968). "Toxicity of cryoprotective agents at 30°." <u>Journal of Pharmacy and Pharmacology</u> **20**(4): 297-301.

Kedem, O. and A. Katchalsky (1958). "Thermodynamic analysis of the permeability of biological membranes to non-electrolytes." <u>Biochim Biophys Acta</u> **27**(2): 229-246.

Kenis, P. J. (1999). "Microfabrication Inside Capillaries Using Multiphase Laminar Flow Patterning." <u>Science</u> **285**(5424): 83-85.

Kleinhans, F. W. (1998). "Membrane permeability modeling: Kedem-Katchalsky vs a two-parameter formalism." Cryobiology **37**(4): 271-289.

Kuo, J. S. and D. T. Chiu (2011). "Controlling mass transport in microfluidic devices." Annu Rev Anal Chem (Palo Alto Calif) **4**: 275-296.

Lagus, T. P. and J. F. Edd (2013). "A review of the theory, methods and recent applications of high-throughput single-cell droplet microfluidics." Journal of Physics D: Applied Physics **46**(11): 114005.

Li, L.-y. (2006). "Numerical simulation of mass transfer during the osmotic dehydration of biological tissues." Computational Materials Science **35**(2): 75-83.

M. Toner, A. A. (2005). Roles of Thermodynamic State and Molecular Mobility in Biopreservation. Tissue Engineering and Artificial Organs, CRC Press**: 1-20.

Maczynski, A., et al. (2007). "IUPAC-NIST Solubility Data Series. 82. Alcohols with Water–Revised and Updated: Part 5. C[sub 8]–C[sub 17] Alcohols with Water." Journal of Physical and Chemical Reference Data **36**(3): 685.

Meryman, H. T. (1971). "Cryoprotective agents." Cryobiology **8**(2): 173-183.

Michael J. Taylor, Y. C. S., Kelvin G.M. Brockbank (2004). "Vitrification in Tissue Preservation: New Developments." 603-641.

Mijatovic, D., et al. (2005). "Technologies for nanofluidic systems: top-down vs. bottom-up--a review." Lab Chip **5**(5): 492-500.

Palasz, A. T. and R. J. Mapletoft (1996). "Cryopreservation of mammalian embryos and oocytes: recent advances." Biotechnol Adv **14**(2): 127-149.

Prot, J.-M., et al. (2012). "Predictive toxicology using systemic biology and liver microfluidic "on chip" approaches: Application to acetaminophen injury." Toxicology and Applied Pharmacology **259**(3): 270-280.

Purcell, E. M. (January 1977). "Life at low Reynolds number." American Journal of Physics **45**(1).

R. Byron Bird, W. E. S., Edwin N. Lightfoot Transport Phenomena, Wiley.

Rubinsky, B. (2003). "Principles of low temperature cell preservation." Heart Fail Rev **8**(3): 277-284.

S. Matsuo, T. M. (1989). "Viscosities of Six 1-Alkanols at Temperatures in the Range 298-348 K and Pressures up to 200 MPa." International Journal of Thermophysics **10**(4).

Santiago, J. G. (2001). "Electroosmotic Flows in Microchannels with Finite Inertial and Pressure Forces." Anal. Chem. **73**: 2353-2365.

Sgro, A. E. and D. T. Chiu (2010). "Droplet freezing, docking, and the exchange of immiscible phase and surfactant around frozen droplets." Lab Chip **10**(14): 1873-1877.

Song, Y. S., et al. (2009). "Microfluidics for cryopreservation." Lab Chip **9**(13): 1874-1881.

Squires, T. M. and M. Z. Bazant (2004). "Induced-charge electro-osmosis." Journal of Fluid Mechanics **509**: 217-252.

Squires, T. M. and S. R. Quake (2005). "Microfluidics: Fluid physics at the nanoliter scale." Reviews of Modern Physics **77**(3): 977-1026.

Stroock, A. D., et al. (2002). "Chaotic mixer for microchannels." Science **295**(5555): 647-651.

Swain, J. E., et al. (2013). "Thinking big by thinking small: application of microfluidic technology to improve ART." Lab Chip **13**(7): 1213-1224.

Teh, S.-Y., et al. (2008). "Droplet microfluidics." Lab on a Chip **8**(2): 198.

Ternström, G., et al. (1996). "Mutual Diffusion Coefficients of Water + Ethylene Glycol and Water + Glycerol Mixtures." Journal of Chemical & Engineering Data **41**(4): 876-879.

Toner, M., et al. (1990). "Thermodynamics and Kinetics of Intracellular Ice Formation during Freezing of Biological Cells." Journal of Applied Physics **67**(3): 1582-1593.

Tong Wang, P. J. W. (2005). Soybean Oil. Bailey's Industrial Oil and Fat Products. F. Shahidi., John Wiley & Sons, Inc.**:** 577-653.

Vian, A. M. and A. Z. Higgins (2014). "Membrane permeability of the human granulocyte to water, dimethyl sulfoxide, glycerol, propylene glycol and ethylene glycol." Cryobiology **68**(1): 35-42.

Warkentin, M., et al. (2008). "Cryocrystallography in capillaries: critical glycerol concentrations and cooling rates." J Appl Crystallogr **41**(Pt 4): 791-797.

Weibel, D. B. and G. M. Whitesides (2006). "Applications of microfluidics in chemical biology." Curr Opin Chem Biol **10**(6): 584-591.

Whitesides, G. M. (2006). "The origins and the future of microfluidics." Nature **442**(7101): 368-373.

Yamaji, Y., et al. (2006). "Cryoprotectant permeability of aquaporin-3 expressed in Xenopus oocytes." Cryobiology **53**(2): 258-267.

Youm, H. W., et al. (2014). "Optimal vitrification protocol for mouse ovarian tissue cryopreservation: effect of cryoprotective agents and in vitro culture on vitrified-warmed ovarian tissue survival." Hum Reprod **29**(4): 720-730.

7. Appendix

7.1 Possible Organic Phase Substances

	Dodecanol		Undecanol		Decanol			Nonanol			2-Ethyl Hexanol		Ocatanol			Cyclooctanol		Soybean Oil
Temperature (°C)	30	40	20	40	20	30	40	20	30	40	20	40	20	30	40	30	40	25
Water Solubility w%	2.87	2.85	3.21	3.09	3.68	3.35	3.48	3.68	3.92	3.94	2.4	2.72	4.35	4.48	4.81	5.18	5.49	0.4
Solubility in Water w%	0.04	0.05	0.03	0.09	0.021		0.026		0.031	0.034	0.125	0.11	0.049		0.065	0.61	0.6	-
Viscosity (mPa.s)	15.91		17.2		11.05			11.7			9.8		10.6			136		58 - 62
Density (g/cm3)	0.8309		0.8298		0.8297			0.8279			0.8344		0.827			0.97		0.917
Melting p. Boiling p. (°C)	24 / 259		19 / 243		6.4 / 232			- 5 / 213			-76 / 184		- 16 / 196			15 / 105		0.6 / >260
Toxicity	Non - Hazardous Toxic to aquatic life		Non - Hazardous Toxic to aquatic life		Non - Hazardous			Toxic by Inhalation Toxic to aquatic life			Target Organ Effects		Non - Hazardous Toxic to aquatic life			Non - Hazardous or Not investigated		Non-Hazardous

Ref.
Solubility: (Maczynski, Shaw et al. 2007)
Viscosity: (S. Matsuo 1989), (Tong Wang 2005)
Other references from (data vary depending on the purity and the manufacturer)
1-United States Library of Medicine – Toxicology Data Network.
2- Sigma Aldrich MSDS forms.